Accepted Manuscript

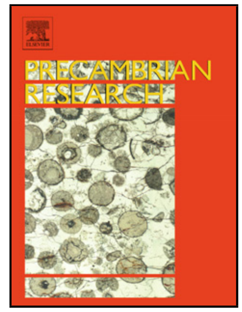

Title: Mesoproterozoic intraplate magmatic 'barcode' record of the Angola portion of the Congo craton: newly dated magmatic events at 1500 and 1110 Ma and implications for Nuna (Columbia) supercontinent reconstructions

Authors: Richard E. Ernst, Eurico Pereira, Michael A. Hamilton, Sergei A. Pisarevsky, José Rodriques, Colombo C.G. Tassinari, Wilson Teixeira, Vitória Van-Dunem

PII: S0301-9268(13)00011-9
DOI: doi:10.1016/j.precamres.2013.01.010
Reference: PRECAM 3703

To appear in: *Precambrian Research*

Received date: 24-7-2012
Revised date: 26-11-2012
Accepted date: 3-1-2013

Please cite this article as: Ernst, R.E., Pereira, E., Pisarevsky, S.A., Rodriques, J., Tassinari, C.C.G., Teixeira, W., Van-Dunem, V., Mesoproterozoic intraplate magmatic 'barcode' record of the Angola portion of the Congo craton: newly dated magmatic events at 1500 and 1110 Ma and implications for Nuna (Columbia) supercontinent reconstructions, *Precambrian Research* (2010), doi:10.1016/j.precamres.2013.01.010

Highlights

- Two new intraplate magmatic events in Angola (Congo craton): 1502 ± 4 Ma & 1110 ± 3 Ma based on U-Pb baddeleyite method.
- These ages plus 1380 Ma Kunene event define Mesoproterozoic magmatic 'barcode' for the Congo- São Francisco craton.
- 1500 and 1380 Ma ages used to reconstruct western margin of the São Francisco (-Congo) craton against northern Siberia.
- The 1110 Ma age is matched with coeval events of Kalahari, Indian, Amazonian cratons in preliminary reconstruction.

Mesoproterozoic intraplate magmatic 'barcode' record of the Angola portion of the Congo craton: newly dated magmatic events at 1500 and 1110 Ma and implications for Nuna (Columbia) supercontinent reconstructions

Richard E. Ernst[a,b], Eurico Pereira[c], Michael A.Hamilton[d], Sergei A. Pisarevsky[e,f], José Rodriques[g], Colombo C.G. Tassinari[h], Wilson Teixeira[h], Vitória Van-Dunem[i]

[a]Ernst Geosciences, 43 Margrave Avenue, Ottawa, Canada, K1T3Y2; Richard.Ernst@ErnstGeosciences.com

[b]Dept. of Earth Sciences, Carleton University, Ottawa, K1S5B6, Canada

[c]Laboratório Nacional de Geologia, Apartado 1089, 4466 – 956 S. Mamede Infesta, Portugal; FEUP, Universidade do Porto, Portugal, euricosousap@gmail.com

[d] Jack Satterly Geochronology Lab., Dept. of Geology, University of Toronto. 22 Russell St. Toronto, ON M5S 3B1,Canada; mahamilton@geology.utoronto.ca

[e]Australian Research Council Centre of Excellence for Core to Crust Fluid Systems (CCFS) and The Institute for Geoscience Research (TIGeR), Department of Applied Geology, Curtin University, GPO Box U1987, Perth, WA 6845, Australia.

[f]School of Earth and Environment, University of Western Australia, 35 Stirling Highway, Crawley, WA 6009, Australia

[g]Laboratório Nacional de Geologia, Apartado 1089, 4466 – 956 S. Mamede Infesta, Portugal; FEUP, Universidade do Porto, Portugal,

[h]Instituto de Geociências, Universidade de São Paulo / CPGeo, Rua do Lago 562, São Paulo, SP, Brasil, CEP 05508-080,

[i]Instituto Geológico de Angola, C. P. 1260, Luanda, Angola

Abstract

In the Angola portion of the Congo Craton, the only Proterozoic large igneous province (LIP) dated prior to this study was the 1380-1370 Ma (Kunene Intrusive Complex and related units). U-Pb TIMS ages on baddeleyite from dolerite sills and gabbro-noritic dykes, has revealed two additional Mesoproterozoic intraplate events: at c. 1500 and c. 1110 Ma, that are each proposed to be part of the plumbing system for LIPs. The identification of these

three Mesoproterozoic magmatic events (c. 1500, 1380, and 1110 Ma) represent an initial magmatic 'barcode' for this portion of Congo Craton (and formerly connected São Francisco Craton), which can be compared with the magmatic 'barcode' record of other blocks to identify former nearest neighbors in the Precambrian supercontinent Nuna (also known as Columbia).

Specifically, a 1502 ± 5 Ma U-Pb TIMS baddeleyite age has been obtained for the prominent Humpata dolerite sill which is part of a wider sill province in SW Angola portion of the Congo Craton. The combined presence of both 1500 Ma and 1380 Ma magmatism in the Congo – São Francisco reconstructed craton is a match with similar ages published for two intraplate magmatic provinces in northern Siberia and suggests a nearest-neighbor relationship in the supercontinent Nuna in which northern Siberia is juxtaposed adjacent to the western São Francisco portion of the reconstructed São Francisco – Congo Craton.

In addition, a precise U-Pb TIMS baddeleyite age of 1110 ± 2.5 Ma was obtained for a prominent NNW-NNE trending gabbro-noritic (GN) dyke swarm in southeastern Angola, but this age is currently unknown in Siberia suggesting that the breakup of Congo-São Francisco Craton from Siberia happened earlier, perhaps in association with the 1380 Ma event. This 1110 Ma age is however, a precise match with that of the Umkondo Large Igneous Province (LIP) of the Kalahari Craton, and also with mafic intraplate magmatism on other blocks such as the Bundelkhand Craton (India) and as the Amazonian Craton. We provisionally consider these three cratons to have been nearest neighbors to the Congo-São Francisco Craton at this time and to have shared this 1110 Ma magmatic event as a LIP node. There is also an age match with the early part of the Keweenawan event (in the interior of the Laurentia); however, on previously discussed paleomagnetic grounds the Keweenawan event is likely to have been distant and unrelated (and on the other side of the Grenville orogen).

1. Introduction

The Congo and São Francisco cratons belong to the approximately 35 main fragments that remain of the latest Archean/ Paleoproterozoic supercontinent (or supercratons) (e.g., Bleeker 2003), and it is generally accepted that these two blocks were joined by about 2.05 Ga and remained together until the ca. 130 Ma breakup of Africa from South America (D'Agrella-Filho et al., 1996; Feybesse et al., 1998). Both Congo and São Francisco cratons consist of

Archean to Paleoproterozoic high-grade gneisses and granite-greenstone supracrustal terranes overlain by Mesoproterozoic to Neoproterozoic platform-type cover (Fig. 1).

The position of these reconstructed cratons (São Francisco plus Congo) in Proterozoic supercontinents Nuna (also known as Columbia) and Rodinia remains speculative (e.g., Meert, 2012; Li et al., 2008, respectively). Their large igneous province (LIP) record provides potential for determining their reconstruction position using the LIP barcode method (Bleeker and Ernst, 2006). The precisely dated LIP barcode record of different crustal blocks can be compared. If two blocks share the same age of LIP magmatism then they may have been nearest neighbors, but it is also possible that they were widely separated blocks that happened to share one age of LIP magmatism (cf., Ernst and Buchan, 2002). However, if multiple ages of LIPs are shared then the likelihood of the blocks being nearest neighbors increases. The Proterozoic LIP barcode record of the São Francisco and Congo cratons is at a preliminary stage of understanding (Fig. 2); there are many recognized mafic dyke swarms and related intrusions that are currently poorly dated or undated.

As a contribution to efforts to determine the position of the São-Francisco-Congo Craton in Nuna and Rodinia supercontinents we have obtained precise U-Pb dates on dolerite and gabbro units in the Bibala-Lubango-Cainde region of Angola in the southwestern branch of the Congo Craton (Fig. 3; Table 1). These are inferred to represent part of the plumbing system of the proposed LIPs (see criteria in Ernst, 2007).

The oldest of these magmatic events (Humpata sill and related mafic intrusions) is intrusive into the volcanic and siliciclastic sequence of the Chela Group (Fig. 3; McCourt et al., 2004; Pereira et al., 2011) that rests unconformably over the Eburnean crystalline basement, without any signs of deformation or metamorphism. Ca 1800 Ma sub-volcanic acid bodies intrude the base of this sedimentary sequence, whereas the undated Humpata olivine-dolerite sills were emplaced at the discontinuity between the top of the Chela Group and the base of overlying dolomitic Leba Formation.

The next oldest important magmatic event is represented by the emplacement of the 1380-1370 Ma (U-Pb) Kunene (Cunene) mafic-ultramafic complex (KIC; e.g., Mayer et al., 2004; McCourt et al., 2004; Druppel et al. 2007; Maier, 2008; Maier et al., 2008) associated with 1376 ± 2 Ma A-type red granites in the southwestern part of the Congo craton. As discussed below coeval ages are present in the eastern part of the Congo craton. Specifically, the KAB (Karagwe-Ankole belt) and KIB (Kibara belt), as recently defined by Tack et al.

(2010) contain bimodal magmatism of 1375 Ma age that include the Kabanga-Musongat-Kapalagulu mafic-ultramafic complex and S-type granites.

In addition, numerous dykes, both sub-ophitic olivine gabbros and gabbro-norites are spread over hundreds kilometers and define lineaments with prominent trends oriented WNW and NNW to NNE, respectively. These are interpreted to represent two distinct generations with poor age constraints (Fig. 3), apart from a cross cutting relationship. The gabbro-norites cut all older sills, mafic dykes and the gabbro anorthosite complex (GC) of Angola-Namibia and are the youngest mafic magmatic event prior to the Pan-African cycle. In addition to these major mafic episodes, there are numerous narrower dykes of dolerite and lamprophyre (mainly spessartite) with undetermined age.

The objective of this study is to contribute to the geologic knowledge of a remote region of the SW Angolan portion of the Congo Craton, revealing the petrochemical character and isotopic age of the poorly dated olivine gabbro and undated gabbro-norite dykes and sills, in order to expand the intraplate magmatic barcode record for this region and contribute to the identification of nearest neighbors to the Congo Craton in Precambrian supercontinent reconstructions (Bleeker, 2003; Bleeker and Ernst, 2006).

2. Geological setting and previous studies on the mafic magmatism in southwestern Angola

More detail is provided below on each of the three age groups of intraplate magmatism that are the focus of this paper (Table 1).

2.1 Olivine dolerite sills and dykes

The sills, usually very weathered, are olivine dolerites emplaced into the Chela Group immediately below the Leba Formation, when it is present. In other regions, to the south and west of the area shown in Fig 3, these dolerites are intruded into quartzites that are presumably related to the Chela Group, or are intruded into other units, such as the gneissic migmatitic complex and the red metaluminous Gandarengos type granite (U-Pb zircon age of 1810 ± 11 Ma; Pereira et al., 2011). The sills are quite well exposed in the southernmost part of the study area (Fig. 3) where they were mapped by Carvalho and Pereira (1969 a, b) and Carvalho and Simões (1971). South of Humpata, extensive sills were reported by Vale et al.

(1973) as occurring principally at the discontinuity between the Chela Group and the Leba Formation. Isotopic K-Ar data of dolerites and subophitic gabbros from Cacula, Quilengues and Caluquembe localities, immediately to the north of the studied region, give ages of 1281 ± 22 Ma and 1175 ± 69 Ma (Silva et al., 1973).

On the Bimbe plateau (the highest elevations of the Chela Mountain (to the south of Fig. 3), there are two small bodies located at the top of the Bruco Formation of the Chela Group (Pereira et al., 2006, 2011). Locally, the Bruco Formation is the highest preserved unit in the Chela Group, given the absence of the overlying units of the Cangalongue and Leba Formations.

In addition, far from the Chela Formation, particularly in the area north of Bibala and east of Lubango, another type of olivine dolerite is observed. It consists of small domal intrusions, rounded in plan-view, that are each about a few dozen meters in diameter, and are intruded into the pre-Eburnean basement. These peculiar bodies are interpreted as pipe-shaped magmatic centers that fed the typical sills of the Chela Mountains, and in those places, the Chela Group formations have been eroded. They are presumably coeval with the dolerite sills reported by Pereira (1973) and Vale et al. (1971).

In addition, numerous olivine dolerite dykes (potentially linked with the sills) have been emplaced following regional fault systems (Andrade, 1962). The largest multi-kilometric dykes (subophitic olivine gabbros) trend consistently WNW (N50°-70°W). These mafic dykes continue to the NW towards the Atlantic coast, having been identified to the north of Fig 2 in Dinde-Lola (Alves, 1968; Vale et al., 1972) and Serra da Neve (Pereira and Moreira, 1978; Pereira et al., 2001). Many smaller dykes (olivine dolerites) also occur in a variety of trends.

2.2 Gabbro-norite dykes

The thick and extensive gabbro-norite (GN) dykes, sometimes more than 200 km in strike length, constitute one of the most prominent features of the regional geology, and have a ubiquitous presence throughout the SW Angola. Torquato and Amaral (1973) had assigned a K-Ar age of c. 800 Ma to similar rocks from the Chiange region (Fig. 3), while in the neighboring region of Caluquembe (region immediately north of Lubango, Fig. 3), K-Ar (whole rock) analyses for the large gabbro-noritic dyke of Bibala yielded ages of 644 ± 27 and 704 ± 17 Ma (Silva et al., 1973), while a K-Ar (plagioclase) age was determined at 788 ±

11 Ma (Silva, 1980). A subsequent Rb-Sr isotopic age of 1119 ± 44 Ma ($^{87}Sr/^{86}Sr$ i = 0.707) (attributed to Vialette, in Carvalho et al., 1979, Carvalho et al., 1987) was widely accepted as a more reliable estimate of the age of the GN suite. Despite the apparent freshness of these rocks, those K-Ar ages are interpreted to have been affected by variable isotopic resetting during the Pan-African orogeny.

2.3 1380 Ma Kunene event

The southern border of the Congo Craton was intruded by the Gabbro-anorthosite Complex (GC) during the Mesoproterozoic (Fig. 3). This Complex is 250 km long and 60 km wide, and represents one of the largest anorthositic batholiths in the world, occupying an area over 15 000 km^2. In early studies, the GC was simply described as a massive anorthosite body (Simpson and Otto, 1960; Vale et al., 1973), but it has also been regarded as layered mafic intrusion (Stone and Brown, 1958; Silva, 1972, 1990, 1992; Carvalho and Alves, 1990). More recent comprehensive studies have included detailed field work, petrographic and tracer isotopic studies, and have established this as a composite suite of massif-type anorthosite (Ashwal and Twist, 1994; Morais et al. 1998; Slejko et al., 2002; Mayer et al., 2004). These authors replaced the long-established name GC (Gabbro-anorthosite Complex) with the name Kunene Complex of SW Angola in order to link it to the Kunene Intrusive Complex (KIC) of the Namibia-Angola border (Menge, 1998; Drüpel et al., 2000, 2007). The current known extent of the KIC, present in both Angola and in adjacent Namibia, indicates that this is the largest mafic complex in Africa. The most precise ages determined for the KIC are 1385 ± 25 Ma (U-Pb TIMS, zircon; Drüppel et al., 2000) for leucogabbronorite and 1371 ± 3 (U-Pb TIMS zircon; Mayer et al., 2004) for a mangerite dyke interpreted to be coeval with the anorthositic rocks. A U-Pb SHRIMP age of 1385 ± 8 Ma was also obtained for zircon from a mangerite dyke intruding massive anorthosites in the Lubango region, (McCourt et al., 2004). Widespread associated "Red Granites" have a similar age of 1376 ± 2 Ma (Drüppel et al., 2007) and these granites have a comingling relationship with some mafic units in southwest Angola, suggesting that these mafic units also belong to the Kunene event.

The 1380 Ma event has a wider extent elsewhere in the Congo Craton. The >500 km Kabanga-Musongati-Kapalagulu mafic-ultramafic belt is located in the Kibaran orogen of the eastern part of the Congo Craton (KAB in Fig. 1). This belt hosts important Ni occurrences (Tack et al., 2010 and references therein). However, the precise age and setting of the

Kabanga-Musongati-Kapalagulu belt is uncertain (Maier, 2008; Ernst et al., 2008 and references therein). The similar-aged S-type granites and mafic-ultramafic intrusions in the Kibaran belt have also been considered synorogenic (e.g. Kokonyangi et al., 2006; see discussion in Maier, 2008). However, more recent U-Pb geochronology argues that this ca. 1375 Ma bimodal magmatism is linked to a regional extensional intraplate event (Tack et al., 2010), which supports the link between these mafic-ultramafic units in the eastern Congo with the anorogenic Kunene Complex of SW Angola and Angola-Namibia, and would indicate a widespread 1380 Ma event in the Congo Craton that would satisfy the criteria of being a LIP (large volume, short duration and intraplate setting; Coffin and Eldholm, 1994; Bryan and Ernst, 2008).

3. Petrography and whole-rock chemical composition

3.1 Dolerite sills in the Chela Group

The olivine dolerite sills closely follow the bedding planes of the Chela Group formations. Normally, the sills are emplaced along the unconformity at the base of the Leba Formation. They are fine to medium-grained, and characterized by an ophitic intergranular texture where plagioclase forms a well-defined network whose interstices are filled by the remaining components, in particular megacrysts of olivine, pigeonite or slightly titaniferous augite and biotite. Plagioclase (An_{50}) is altered to phyllitic, argillaceous and carbonaceous materials, and augite is locally altered to amphibole of the tremolite-actinolite series. When unweathered, olivine is often euhedral; elsewhere, it shows reaction with the matrix and gives rise to crown-shaped textures, bordered by clinopyroxene, chromite and biotite. Occasionally, olivine is completely altered to serpentine minerals or fringed and intergrown with chromite and magnetite. Accessory minerals include magnetite, titanomagnetite, apatite and titanite. Secondary minerals include fibrous amphibole, antigorite, leucoxene, carbonates, chlorite and epidote.

In general, the dolerite sills show varying degrees of hydrothermal alteration, which may be linked to proximity to the Kaoko Belt of Namibia. The Kaoko Belt, trending NNW-SSE along the coastline of Namibia and continuing to the SW of Angola (Seth et al., 1998; Passchier et al., 2002; Goscombe and Gray, 2007; 2008) is the NW branch of the Damara belt

(Kröner, 1982; Martin, 1983; Miller, 1983; Prave, 1996). In Fig 1, the Kaoko Belt is marked as a Pan-African Belt (650-550 Ma).

Although the sills are not deformed, their major element and large-ion lithophile (LIL) trace element chemical compositions have likely been affected by fluid alteration (see Tables 2, 3, Fig. 4). However, using only the high field strength elements (HFS), interpreted to be relatively immobile under hydrothermal conditions (Winchester and Floyd, 1977; Pearce and Norry, 1979), we conclude that the dolerite sills were emplaced with sub-alkaline basaltic compositions (Fig. 4). These rocks have relatively high levels of Rb, Th, U and K, but low values of Nb-Ta, Zr, Hf, and Ti relative to primitive mantle (normalized multi-element values of Sun and McDonough, 1989); REE levels are between 9 and 100 times chondritic levels. The data plot (Table 3) in the within-plate basalt field of the diagram Zr/Y-Zr (Pearce and Norry, 1979), and the transition field C of the Zr/4-Y-Nb*2 diagram (Meschede, 1986). Steep REE patterns (La_N/Yb_N= 4-6), variable negative or slightly positive Eu anomalies (Eu/Eu*=0.7-1.1, calculated according to Taylor and McLennan, 1985) and values for other parameters, are, Th/Nb (0.1-1.2), La/Nb (1.8-2.9), Zr/Nb (14.5-21.6) and Hf/Th (0.38-0.48 with an anomalous value of 3.8). Collectively the geochemistry is indicative of an intraplate environment, low fractionation and slightly alkaline character.

3.2 Gabbro-norite (GN) dykes (NNE-NNW trending)

The gabbro-norite dykes are typically coarse to medium grained with a sub-ophitic to ophitic texture, where labradorite (An_{64}) and enstatite form an interlocking network of crystals with insterstices filled by magnetite, pigeonite, quartz and micropegmatite. The accessory minerals include quartz and K-feldspar in micrographic association, biotite, green hornblende, apatite, zircon and titanomagnetite. Bronzite, chlorite, fibriform amphibole alteration of pyroxene, leucoxene and epidote are the secondary minerals. This general mineralogy led to the initial classification of these rocks as *norites*, the petrographic term used for large NNW-trending dykes in SW Angola by Simões (1971); these are now referred to the GN (gabbro-norite) suite.

The incipient metamorphism resulting from the proximity of the Kaoko belt of Namibia and the hydrothermal and meteoric alteration processes, observed in the GN, can cause chemical variation in the concentration of many elements, especially in the major and the large-ion lithophile trace elements (LIL) (Tables 2, 4). The abundance of immobile incompatible elements confirms a basaltic composition for the gabbro-norite suite (Fig. 5; Winchester and Floyd, 1977). On the normalized multi-element diagram they exhibit higher enrichment in Rb, Ba, Th, U and K than in Nb-Ta, Sr, Ti, Y, while REE levels are between 7 and 100 times chondrite (Fig. 5). A general LREE enrichment, medium steep REE pattern (La_N/Yb_N= 4-7), variable negative or slightly positive Eu anomalies (Eu/Eu*=0.8-1.1) and other parameters, including Th/Nb (0.1-1.1), La/Nb (1.8-8.2) and Zr/Nb (11.8-27.7) are indicative of an intraplate environment, slight fractionation and various degrees of magmatic crustal contamination. Also, the general geochemical characteristics (Table 3), the projection on the tholeiitic field of the diagram (ALK)- MgO-FeOt (Irvine and Baragar, 1971) and the affinity of most samples plotted to the field **C** of the Zr/4-Y-Nb*2 diagram (Meschede, 1986), combined with the low content of Nb-Ta and Ti - all clearly indicate a domain of within-plate tholeiites. In conclusion, the petrochemical data presented for the GN Suite are suggestive of within-plate magmas, revealing slight contamination during residency and emplacement in Congo Craton crust.

4. New U-Pb TIMS ages

4.1 Analytical Methods

Sample processing and isotopic analysis were carried out at the Jack Satterly Geochronology Laboratory at the University of Toronto. Protocols for baddeleyite (ZrO_2) mineral separation and for isotope dilution thermal ionization mass spectrometry (ID-TIMS) for U-Pb analysis followed those outlined in detail by Hamilton and Buchan (2010). Uranium-lead isotopic data are provided in Table 5, and presented in graphical form in Figure 6 (A, B). Uranium decay constants used in age calculations are those of Jaffey et al. (1971). Error ellipses shown in concordia diagrams, and uncertainties on ages described in the text are all presented at the 2σ level (95% confidence). Data were plotted and ages were calculated using the Microsoft Excel Add-in Isoplot/Ex v. 3.00 of Ludwig (2003).

4.2 Dolerite sills of Chela Group

A dolerite sill was collected for dating approximately 25 km SSE of Humpata, Angola (sample 356-56; Fig. 3b). At the sampling site, the Humpata sill is about 50 m thick; material for dating was collected from the coarser-grained, interior portion of the sill. U-Pb analyses were carried out on three fractions of baddeleyite, each comprising between 4-5 pale- to medium-brown, fresh blades and blade fragments. Results range from 2.9-4.2% discordant, but are strongly collinear ($^{207}Pb/^{206}Pb$ ages range from 1502.8 to 1500.0 Ma).

Free regression of the data for all three fractions results in a lower intercept within error of the origin, suggesting only recent Pb-loss (possibly due to alteration of submicroscopic zircon overgrowths); therefore a linear regression was anchored at 0 Ma, yielding an upper intercept age at 1501.5 ± 3.6 Ma (2σ; 77% probability of fit) (Table 5, Fig. 6a). We interpret the age of 1502 ± 4 Ma to represent the best estimate of the age of emplacement and crystallization of the olivine dolerite sill into the Chela Group sediments.

4.3 Gabbro-norite (GN) dykes

Sample 356-17 (Fig. 3b) was collected from a NNW-trending gabbro-norite dyke, approximately 17 km SW of the village of Chibia, Angola. The dyke is unmetamorphosed, subvertical, up to 50 m thick, and extends for more than 200 km along strike. The host rocks at the sampling site include Eburnean peraluminous granites (ca. 2.0 Ga) and the volcano-sedimentary members of the Chela Group. Here, the dyke is ~ 35 m thick and was sampled from the coarsest interior portion. This medium-grained subophitic gabbro-norite yielded abundant, fresh, pale- to medium-brown, elongate to stubby broken blades of baddeleyite ranging up to approximately 80 microns in the longest dimension. The analyses for three fractions, comprising 5-7 grains each, are slightly clustered, ranging from 1.2-1.6% discordant (Table 5). Assuming a recent, simple Pb-loss history as for sample 356-56, the data yield an average $^{207}Pb/^{206}Pb$ age of 1110.3 ± 2.5 Ma (Fig. 6b). We interpret this age to closely reflect the age of emplacement and crystallization of this NNW-trending gabbro-norite dyke and associated NNW-NNE trending swarm.

5. Regional barcode significance

5.1 1500 Ma Large Igneous Province

Our data is the first indication of a ca. 1500 Ma magmatic event in the Congo Craton. The specific age is from the sills in the Humpata Plateau. However, there are other sills elsewhere in SW Angola that could be related. Specifically, these include the sills of the Ompupa, Otchinjau and Cahama regions (Fig. 3), which are intrusive into the quartzitic sequence related to the Chela Group (e.g., Carvalho, 1984; Carvalho and Alves, 1990, 1993).

Similar U-Pb ages have also been recently obtained in the northern portion of the São Francisco craton. For example, the Curaçá dyke swarm and the Chapada Diamantina dykes and sills, which are considered to be related to a distinct intraplate event, have recently been dated at 1503-1508 Ma (Silveira et al., 2012). The presence of c. 1500 Ma extensional mafic magmatism in both blocks (Congo and São Francisco cratons) is significant since both blocks are generally assumed to have been joined during the Neoproterozoic and Mesoproterozoic – a conclusion supported by regional geologic correlations – and to have separated only during the breakup of the Gondwana supercontinent and the opening of the Atlantic ocean (e.g., De Waele et al. 2008, and references therein). Thus, in a combined Congo - São Francisco Craton, a ca. 1502-1508 Ma magmatic event would have defined a very wide extent, at least 1500 km across (Fig. 1). Because of the large expanse of this igneous activity, its probable short duration (with a possible range of 1502-1508 Ma) and its intraplate setting, it should likely be considered as a LIP (cf. Bryan and Ernst, 2008).

5.2 1110 Ma event

The 1110 ± 2.5 Ma Gabbro-Norite dyke belongs to a roughly linear swarm (Figs. 1 and 3) that is close to, and obliquely intersects, the southwestern margin of the Congo Craton (Fig. 1). The full extent of the 1110 Ma event within the Congo-São Francisco Craton remains to be defined, but we suspect it is widespread given its presence on several other crustal blocks that we propose to have been formerly adjacent (see below).

Dolerite dykes (Salvador, Ilheus, and Olivença swarms) of the eastern margin of the São Francisco Craton (e.g., Ernst and Buchan, 1997), were previously dated, locally, by ^{40}Ar-^{39}Ar methods at ca. 1100-1000 Ma (Renne et al., 1990). On this basis, those giving the older ages could have been interpreted to be coeval with the GN dykes described here. However, recent U-Pb dating now suggests that all the dykes of these swarms are ca. 925 Ma in age (Heaman, 1991, Evans et al., 2010), and therefore are unrelated to the GN dykes.

6. Summary and Reconstruction Implications

Our U-Pb dating of units in the Congo craton is a step forward in efforts to complete the LIP barcode for this craton (Fig. 2) for purposes of global reconstructions (cf. Bleeker and Ernst, 2006). There are now three major barcode events identified in the western part of the Congo-São Francisco Craton - the previously known 1380-1370 Ma Kunene Intrusive event, and two new events identified at 1508-1502 Ma (this study; Silviera et al., 2012), and at 1110 Ma (this study).

6.1 1500 and 1380 Ma events

These two older events, 1508-1502 Ma and 1380 Ma may be associated with one of the stages of the breakup of the Nuna supercontinent (Meert, 2012 and references therein), and the 1380 Ma event, in particular, is found on many crustal blocks (e.g., Ernst et al., 2008). These two events represent 'barcode' lines (Bleeker, 2003; Bleeker and Ernst 2006) that can be compared with the record on other blocks to identify which have matching barcodes and can therefore have been former nearest neighbors to the Congo-São Francisco Craton inside the Nuna supercontinent.

In comparison with the global LIP record for this time period (Ernst et al., 2008) the most compelling match is with the Siberian Craton, suggesting a possible nearest neighbor relationship (Fig. 2). For example, two intraplate magmatic events are identified in northern Siberia with ages of 1505 Ma and 1380 Ma (Ernst et al., 2000; Ernst et al., 2008; Khudoley et al. 2007; Gladkochub et al., 2010). The 1500 Ma event is represented by the E-W trending Kuonamka dykes (1503 ± 5 Ma; U-Pb TIMS, baddeleyite) in the central Anabar shield. In addition, the Riphean succession on the northern margin of the Anabar shield contains mafic sills, one of which is dated by the Sm-Nd isochron method at 1513 ± 51 Ma (Veselovskiy et al. 2006), while sills in the the Olenek uplift to the east of the Anabar shield are dated at 1473 ± 24 Ma (Wingate et al., 2009).

The 1380 Ma event is defined based on a 1384 ± 2 Ma (U-Pb TIMS, baddeleyite) age on a dyke of a NNW-trending Chieress swarm in the eastern Anabar shield (Ernst et al., 2000). A dolerite dyke dated at 1339±54 Ma Sm-Nd in the Sette Daban region of the Verkoyansk belt of southeastern Siberia may also belong to this 1380 Ma event (Khudoley et al., 2007). In addition, two sills in the Central Taimyr Accretionary Belt to the north of the Siberia craton yield similar U-Pb ages of 1374 ± 10 Ma and 1348 ± 37 Ma (U-Pb baddeleyite on a Cameca 1270; Khudoley et al., 2009). However, the relationship of this region to the Siberian craton is uncertain (cf. Vernikovsky, 1996). In particular, Neoproterozoic ophiolites are found in Central Taimyr implying oceanic affinity of its composing microterranes (Vernikovsky and Vernikovskaia, 2001). We provisionally suggest that (during the Mesoproterozoic) the

Congo-São Francisco Craton (western margin?) might have been proximal to the northern margin of the Siberian Craton.

The dated Chieress dyke in Siberia has been studied paleomagnetically by Ernst et al. (2000), providing a VGP (virtual geomagnetic pole) of 4°N and 258°E (A_{95}=7°) for Siberia at 1384 ± 2 Ma. Piper (1974) reported a paleomagnetic pole for the Kunene (Cunene) Anorthosite Complex of 3°S and 255°E (A_{95}=17°). At the time of the original publication, the Kunene Complex was loosely dated between 2600 and 1100 Ma, so this paleopole was rarely mentioned in subsequent paleomagnetic compilations. Recently, however, the Complex has been more precisely dated at 1385-1375 Ma (see discussion above), so this pole could be used to better constrain a Siberia - São Francisco reconstruction. Fig. 7 shows the closest permissive paleomagnetic fit of Siberia and Congo-São Francisco at 1380 Ma. However, this paleomagnetic constraint should be treated with caution, as the Chieress VGP represents just one dyke and may reflect the position of a 1380 Ma geomagnetic pole rather than a geographic pole. The LIP barcodes of Siberia and Congo-São Francisco allow their juxtaposition at 1500 Ma, but we cannot test this paleomagnetically, because there are no reliable ca. 1500 Ma paleomagnetic poles yet available for the Congo or São Francisco cratons. Positions of Laurentia and Baltica in this reconstruction are based on paleomagnetic data from these continents and on the paleomagnetically and geologically valid suggestion that Laurentia, Baltica and Siberia were parts of a coherent Nuna supercontinent between ca 1500-1270 Ma (Wingate et al., 2009; Pisarevsky and Bylund, 2010).

However, the closeness of fit of Siberia and Laurentia is under debate (Fig. 7). These authors (Wingate et al., 2009; Pisarevsky and Bylund, 2010) prefer a gap between Siberia and northern Laurentia filled by another as yet unidentified crustal block. However, a tight fit (with no gap) is favoured (Ernst and Bleeker, 2011; Bleeker and Ernst 2011) on the basis of numerous intraplate magmatic barcode matches between southern Siberia and northern Laurentia between 1900 and 725 Ma (1900 Ma, 1870 Ma, 1750 Ma, 1700 Ma, 1640 Ma, 1380 Ma, 780 Ma and 725 Ma) favouring a nearest neighbor relationship through this interval. A complication for this close fit interpretation is that the 1270 Ma Mackenzie event is widespread in northern Laurentia, but has not yet been found in Siberia. Also, no analogue of the ca. 1000 Ma magmatism in Sette Daban (Siberia, Rainbird et al., 1998) has been found in Laurentia. Evans and Mitchell (2011) find paleomagnetic support for a close fit of southern Siberia and northern Laurentia between 1.9 and 1.2 Ga. In the reconstruction shown in Figure 7, if the gap between Siberia and Laurentia is closed, then the southern Angola portion of the Congo Craton could be juxtaposed against similar ca. 1380 Ma-aged magmatism in Baltica and northern Greenland (e.g., Ernst et al., 2008). Importantly, the Volga Uralia region of Baltica hosts the widespread ca. 1380 Ma Mashak event (Puchkov et al., 2012). Also nearby in a close reconstruction would be the Midsommerso – Zig Zag Dal ca. 1380 Ma magmatism of northern Greenland (Upton et al., 2005). Further geochronological and paleomagnetic studies are required to determine whether the gap between Siberia - Congo-São Francisco and Laurentia – Baltica shown in Figure 7 existed or not.

Here we consider some of the geological evidence in support of the Mesoproterozoic reconstruction proposed in Figure 7. There is evidence for passive margin environments in the NE Siberia that commenced sometime in the Mesoproterozoic, but it remains difficult to date this event more precisely (Pisarevsky and Natapov, 2003; Pisarevsky et al., 2008). The western border of the São Francisco Craton was a passive margin, facing a large ocean basin in early Neoproterozoic times (Fuck et al., 2008). The timing of opening of this ocean is not constrained, but its closure was under way by ca. 900 Ma (Pimentel and Fuck, 1992; Pimentel et al., 2000). This also implies a period of late Mesoproterozoic rifting and breakup.

Further insight comes from the geometry of the dyke swarms. As noted in Silveira et al. (2012), the convergence of the ca. 1500 Ma dykes toward the western margin of the São Francisco craton would be consistent with a plume centre on or toward the western margin of that craton (Fig. 1). Within the uncertainties of the reconstruction fit, this plume centre could also link with the eastern end of the Kuonamka swarm of the northern Siberian Craton (Fig. 7), and could indicate a breakup (or attempted breakup) with a block formerly attached to the NE margin of the Siberian Craton. Furthermore, if the poorly-dated WNW trending olivine dolerites of SW Angola (Fig. 3b, and discussed above) are matched with the olivine dolerite sills dated herein as 1500 Ma, then they could also be used as a geometric element. As shown in Figure 7, they also align toward the proposed 1500 Ma plume centre.

The 1100 Ma global paleogeographic reconstruction of Li et al. (2008), and all other Late Mesoproterozoic and Neoproterozoic reconstructions of which we are aware, show Congo-São Francisco and Siberia cratons far apart from each other. Thus, if our reconstruction (Fig. 7) is correct, this implies that the timing of breakup between these two cratons occurred sometime between 1380 Ma and 1100 Ma.

5.2 1110 Ma event

A third magmatic 'barcode line' now identified for the Angola portion of the Congo Craton is that provided by the 1110 Ma age on the GN dykes. This event may not be relevant to the Nuna supercontinent because the first stage of its breakup had probably already occurred, perhaps associated with the 1380 Ma LIP event(s) which is known from many dispersed crustal blocks (e.g., Li et al., 2008; Ernst et al., 2008) as discussed above. In this scenario, the 1110 Ma event would be occurring in the transition from rupture and fragmentation of the Nuna supercontinent to assembly of the Rodinia supercontinent (e.g., Li et al., 2008).

The 1110 Ma age of this major dyke swarm (Fig. 3) was unexpected and represents a precise barcode match with several other LIPs around the world (cf. Ernst et al., 2008; Figs. 2 & 8). The most notable match is with the Umkondo event of the Kalahari Craton (Hanson et al., 1998, 2004, 2006) where ID-TIMS dating on zircons and baddelyites indicate that the majority of magmatism is bracketed between ca. 1112-1106 Ma. The Mahoba suite of ENE-WSW trending dykes in the Bundelkhand Craton of northern India are also dated, by laser ablation ICP-MS U-Pb methods, at ca. 1110 Ma (Pradhan et al., 2012). A third (newly recognized) locus of 1110 Ma magmatism occurs in the Bolivian portion of the Amazonian craton (Hamilton et al., 2012). The Keweenawan event of the Mid-Continent region of Laurentia has an age range of 1115-1085 Ma (e.g., Heaman et al., 2007) which overlaps with the 1110 Ma age reported here. Two other LIP events (e.g., Ernst et al., 2008), the ca. 1076 Ma Warakurna event of Australia (e.g., Wingate et al., 2004) and the ca. 1100-1069 Ma Southwest USA diabase province (e.g., Ernst et al., 2008; Bright et al., 2012), are probably too young to be related.

A preliminary reconstruction of these blocks that contain 1110 Ma magmatism is offered in Figure 8. The paleolatitude and paleo-orientation of the Indian craton at 1110 Ma is constrained in the study of Pradhan et al. (2012) on the ENE–WSW trending Mahoba suite of dykes of India. The paleolatitude and paleo-orientation of the Kalahari craton at 1110 Ma is based on the paleomagnetism of the Umkondo LIP (Gose et al., 2006). The paleomagnetism of Amazonia at this time is unconstrained as is the position of Angola (Congo-São Francisco Craton). India and Kalahari are shown in their correct paleolatitudes and orientation while Amazonia and Angola (Congo-São Francisco Craton) are arranged to be in proximity in order to satisfy the 1110 Ma LIP barcode match. Amazonia is kept linked with the West African Craton as in the Rodinia reconstruction of Li et al. (2008), in the Gondwana/Pangea fit. While Figure 8 is not a definitive reconstruction it does satisfy the above-mentioned constraints.

This is offered as a provisional match, but additional geochronology and paleomagnetic study of the LIP events on each block plus comparison of the basement geology is required to test and improve this reconstruction. On the other hand, the Keweenawan event of Laurentia lay on the opposite side of the Grenville orogeny and probably represents an independent 1110 Ma plume and LIP. This is supported by paleomagnetic data from Laurentia (Table 1 in Pisarevsky et al., 2003) and Kalahari, which suggest a large distance between them (see also Powell et al., 2001; Hanson et al., 2004; Jacobs et al., 2008). Pb isotope studies (Loewy et al., 2011) indicate that the Keweenawan (Laurentia) and Umkondo (Kalahari) LIPs originated from isotopically distinct Pb reservoirs, supporting the notion of a significant separation of Laurentia and Kalahari at ca. 1100 Ma.

Conclusion

Three Mesoproterozoic intraplate magmatic barcode events at 1500, 1385 and 1110 Ma are now recognized for the São Francisco and Congo cratons which were connected from at least ca. 2000 Ma to the opening of the southern Atlantic ocean at ca. 130 Ma. The previously recognized 1380-1370 Ma LIP is widespread in the Congo Craton and includes the Kunene gabbro anorthosite and related units of Angola (SW Congo craton) and also bimodal magmatism in the eastern part of the Congo Craton.

Two new events are recognized based on U-Pb ID-TIMS dating of baddeleyite from dolerite samples of SW Angola (1500 and 1110 Ma). A 1502 ± 5 Ma age obtained for the Humpata olivine dolerite sill is considered applicable to other sills in the region, and is equivalent to U-Pb ages obtained for mafic dykes in the São Francisco Craton (Silveira et al., 2012). In addition, a 1110 ± 2.5 Ma age has been obtained for the prominent 200 km long NNW-NNE-trending GN (gabbro-norite) swarm of SW Angola.

The exact match of the 1500 and 1380 Ma events of Congo-São Francisco Craton with the northern part of the Siberian Craton suggest a nearest neighbor relationship and a reconstruction is shown based on preliminary paleomagnetic constraints from the literature and from a speculative radiating dyke swarm pattern.

The 1110 Ma Gabbro-Norite swarm of Angola is a precise match with the Umkondo LIP of the Kalahari Craton, and also with mafic magmatism on other blocks such as the Bundelkhand Craton (India) and the Amazonian Craton. We provisionally consider these three cratons to have been nearest neighbors to the Congo-São Francisco Craton at this time and to have shared this 1110 Ma magmatic event and we offer a preliminary reconstruction. There is also an age match with the early part of the Keweenawan event (in the interior of the Laurentia); however, on paleomagnetic and geochemical grounds the Keweenawan event is likely to have been distant and unrelated (and on the other side of the Grenville orogen).

Acknowledgements

We thank Simon Johnson, Vladimir Pavlov and an anonymous reviewer for their constructive suggestions which improved the manuscript, and Randall Parrish for editorial handling. The support for this research was obtained from "Instituto Português de Apoio ao Desenvolvimento" (IPAD), "Laboratório Nacional de Energia e Geologia" (LNEG), Portugal, and from "Centro de Pesquisas Geocronológicas" of the São Paulo University, Brasil. To the General Director and Technical Director of the "Instituto Geológico de Angola" we thank the field work support. This is contribution 221 from the ARC Centre of Excellence for Core to Crust Fluid Systems, and TIGeR publication 436 and also publication #24 of the LIPs-Supercontinent Reconstruction Project (http://www.supercontinent.org).

APPENDIX:

Analytical procedures - Major, minor and trace element geochemistry

The whole-rock chemical compositions, listed in Tables 3 and 4 were obtained at "Laboratório Nacional de Energia e Geologia" (LNEG) (Porto-Portugal). Major and minor elements were analyzed on fused glass discs and pressed powder pellets (produced in a Herzog HTP 40) by X Ray Fluorescence Spectrometry (XFR), with dispersing λ PW2404-PANalytical. For the REE and some trace elements of small ionic radius, the samples were analyzed by Inductively Coupled Plasma - Mass Spectrometry (ICP-MS) using sample decomposition and sintering with Na_2O_2. The results were validated using standards of the Geopt Proficiency-testing Program and the precision of analyses is detailed in Machado and Santos (2006).

References

Alves, C.A. Matos, 1968 – Estudo geológico e petrológico do maciço alcalino-carbonatítico do Quicuco. Junta de Investigação do Ultramar, Lisboa.

Andrade, M.M., 1962. Sobre a ocorrência de doleritos com augite, enstatite e micropegmatite no Sudoeste de Angola. Estudos Científicos oferecidos em homenagem ao Prof. Doutor J. Carrington da Costa. Memória da Junta de Investigação do Ultramar, Lisboa, 495-306.

Araújo, A.G., Perevalov, O.V., Jukov, R.A., 1988. Carta Geológica de Angola, Escala: 1:000 000. Instituto Nacional de Geologia, Angola.

Ashwal, L.D., Twist, D., 1994. The Kunene Complex, Angola / Namibia: a composite massif-type anorthosite complex. Geological Magazine 131, 579-591.

Bleeker, W. 2003. The late Archean record: a puzzle in ca. 35 pieces. Lithos 71, 99-134.

Bleeker W, Ernst R.E., 2006. Short-lived mantle generated magmatic events and their dyke swarms: The key unlocking Earth's paleogeographic record back to 2.6 Ga. *In* Dyke Swarms - Time Markers of Crustal Evolution. *Edited by* E. Hanski, S. Mertanen, T. Rämö, and J. Vuollo. Taylor and Francis/Balkema, London, pp. 3-26.

Bleeker, W., Ernst, R.E., 2011. Does the Slave craton continue into southern Siberia: comparison of their large igneous province (LIP) records. In: Fischer, B.J., and Watson, D.M. (compilers), 39th Annual Yellowknife Geoscience Forum Abstracts. Northwest Territories Geoscience Office, Yellowknife NT. YKGSF Abstracts Volume 2011, pp. 22-23.

Bright, R.M., Amato, J.M., Denyszyn, S.W., Ernst, R.E. B., Amato, J., 2012. U-Pb geochronology and isotope geochemistry of ~1.1 Ga diabase dikes and sills in the southwest U.S.: Implications for Rodinia reconstructions" Rocky Mountain Section - 64th Annual Meeting (9-11 May 2012), Abstract No: 203717 GSA Abstracts with Programs Vol. 44, No. 6.

Bryan, S.E. and Ernst, R.E. 2008. Revised Definition of Large Igneous Provinces (LIPs). Earth-Science Reviews 86, 175-202.

Carvalho, H., 1984. Estratigrafia do Precâmbrico de Angola. Garcia de Orta, Lisboa 7 (1-2), 1-66.

Carvalho, H., Alves, P., 1990. Gabbro-anorthosite Complex of SW Angola / NW Namíbia. Notes about the general geology. An essay of genetic interpretation. Comunicações do Instituto de Invstigação Científica Tropical, Série Ciências da Terra nº 2, 66 pp.

Carvalho, H., Alves, P., 1993. The Precambrian of SW Angola and NW Namibia. Comunicações do Instituto de Invstigação Científica Tropical, Série Ciências da Terra nº 4, 38 pp.

Carvalho, H., Crasto, J., Silva, Z.C. and Vialette, Y., 1987 – The Kibarian cycle in Angola: a discussion. In: Bowden, P., Kinnaird, J., (Eds.), African Geology Reviews, Geological Journal, 22 (1), 85-102.

Carvalho, H., Fernandez, A., Vialette, Y., 1979. Chronologie absolue du Précambrien du Sud-ouest de l'Angola. Comptes Rendus de l'Académie des Sciences, Paris, v. 288, 1647-1650.

Carvalho, H., Pereira, E., 1969a. Carta Geológica de Angola, à escala 1:100 000. Notícia Explicativa da Folha 377 (Vila de Almoster). Serviço de Geologia e Minas, Angola, 47 pp.

Carvalho, H., Pereira, E., 1969b. Fenómenos de bordadura e metamorfização dos gabros na região de Vila de Almoster (Angola, África Ocidental Portuguesa). Serviço de Geologia e Minas, Angola, Boletim, 20, 25-53.

Carvalho, H, Simões, M.C., 1971. Carta Geológica de Angola, à escala 1:100 000. Notícia Explicativa da Folha 376 (Macota). Serviço de Geologia e Minas, Angola, 53 pp.

Coffin, M.F., and Eldholm, O. 1994. Large igneous provinces: crustal structure, dimensions, and external consequences. Reviews of Geophysics, **32**: 1-36.

D'Agrella Filho, M.S.; Feybesse, J.L, Prian, J.P., Dupuis, D., N‟Dong, J.E., 1996. Paleomagnetism of Precambrian rocks from Gabon, Congo craton, Africa. Journal of African Earth Sciences 22, 65-80.

De Waele, B., Johnson, S.P., Pisarevsky, S.A., 2008. Palaeoproterozoic to Neoproterozoic growth and evolution of the eastern Congo Craton: Its role in the Rodinia puzzle. Precambrian Research 160, 127-141, doi: 10.1016/j.precamres.2007.04.020.

Drüppel, K., Littmann, S., Okrusch, M., 2000. Geo und isotopen- chemische Untersuchungen Anorthosite des Kunene-Intrusiv-Komplex (KIC) in NW-Namibia. Berichte der Deutschen Miralogischen Gesellschaft Beiheft zum European Journal Mineralogy 12, 37.

Drüppel, K., Littmann, S., Romer, R.L., Okrusch, M., 2007. Petrology and isotopic geochemistry of the Mesoproterozoic anorthosite and related rocks of the Kunene Intrusive Complex, NW Namibia. Precambrian Research 156, 1-31

Ernst, R.E., 2007. Mafic-ultramafic Large Igneous Provinces (LIPs): Importance of the pre-Mesozoic record. Episodes 30 (2): 108-114.

Ernst, R.E., and Buchan, K.L., 1997. Giant radiating dyke swarms: their use in identifying pre-Mesozoic large igneous provinces and mantle plumes. *In*: Large Igneous

Provinces: Continental, Oceanic, and Planetary Volcanism. *Edited by* J. Mahoney and M. Coffin. Geophysical Monograph Series, v. 100. American Geophysical Union, pp. 297- 333.

Ernst, R.E.**,** Buchan, K.L., 2002. Maximum size and distribution in time and space of mantle plumes: evidence from large igneous provinces. In: Condie, K.C., Abbott, D., Des Marais, D.J. (eds.) Superplume Events in Earth’s History: Causes and Effects: Journal of Geodynamics (Special Issue) 34, 309-342 [Erratum: J. Geodynamics, (2002) 34, 711-714].

Ernst, R.E., Bleeker, W., 2010. Large igneous provinces (LIPs), giant dyke swarms, and mantle plumes: significance for breakup events within Canada and adjacent regions from 2.5 Ga to present. Canadian Journal of Earth Sciences 47, 695-739, doi: 10.1139/E10-025.

Ernst, R.E., Bleeker, W. 2011. Comparing the Large Igneous Province records of northern Canada and southern Siberia: Evidence for a ca. 1.9 to 0.7 Ga nearest neighbor relationship. International Symposium: LIPs of Asia: Mantle Plumes and Metallogeny, August 20-23, 2011, Irkutsk, Russia, p. 75-78, http://lip-asia.com/

Ernst, R.E., Buchan, K.L., Hamilton, M.A., Okrugin, A.V., Tomshin, M.D., 2000. Integrated paleomagnetism and U–Pb geochronology of mafic dikes of the Eastern Anabar shield region, Siberia: implications for Mesoproterozoic paleolatitude of Siberia and comparison with Laurentia. Journal of Geology 108, 381–401.

Ernst, R.E, Wingate, M.T.D., Buchan, K.L., Li, Z.X., 2008. Global record of 1600-700 Ma Large Igneous Provinces (LIPs): Implications for the reconstruction of the proposed Nuna (Columbia) and Rodinia supercontinents. Precambrian Research 160, 159-178.

Evans, D.A.D., Mitchell, R.N., 2011. Assembly and breakup of the core of Paleoproterozoic–Mesoproterozoic supercontinent Nuna. Geology, v. 39, p. 443-446, doi: 10.1130/G31654.1

Evans, D.A.D., Heaman, L.M., Trindade, R.I.F., D'Agrella-Filho, M.S., Smirnov, A.V., and Catelani, E.L., 2010. Precise U-Pb Baddeleyite Ages from Neoproterozoic Mafic Dykes in Bahia, Brazil, and their Paleomagnetic/Paleogeographic Implications, AGU Brazil Abstract, GP31E-07 American Geophysical Union, Joint Assembly, Meeting of the Americas, Iguassu Falls, August 2010.

Feybesse, J.L., Johan, V., Triboulet, C., Guerrot, C., Mayaga-Mikolo, F., Bouchot, V., Eko N‟dong, J., 1998. The West Central African belt: a model of 2.5-2.0 Ga accretion and two-phase orogenic evolution. Precambrian Research 87, 161-216.

Fuck, R.A., Brito Neves, B.B., Schobbenhaus, C., 2008. Rodinia descendants in South America. Precambrian Research 160, 108–126.

Gladkochub, D.P., Pisarevsky, S.A., Donskaya, T.V., Ernst, R.E., Wingate, M.T.D., Söderlund, U., Mazukabzov, A. M, Sklyarov, E.V., Hamilton, M. A., Hanes, J.A., 2010. Proterozoic mafic magmatism in Siberian craton: An overview and implications for paleocontinental reconstruction. Precambrian Research 183, 660-668, doi: 10.1016/j.precamres.2010.02.023

Goscombe, B., Gray, D.R., 2007. The Coastal Terrane of the Kaoko Belt, Namibia: Outboard arc-terrane and tectonic significance. Precambrian Research 155, 139-158.

Goscombe, B., Gray, D.R., 2008. Structure and strain variation at mid-crustal levels in a transpressional orogen: A review of Kaoko Belt structure and the character of West Gondwana amalgamation and dispersal. Gondwana Research 13, 45-85.

Gose, W.A., Hanson, R.E., Dalziel, I.W.D., Pancake, J.A., Seidel, E.K., 2006. Paleomagnetism of the 1.1 Ga Umkondo large igneous province in southern Africa. Journal of Geophysical Research 111, B09101, doi:10.1029/2005JB003897.

Gray, D.R., Foster, D.A., Goscombe, B., Passchier, C.W., Trouw, R.A., 2006. $^{40}Ar/^{39}Ar$ thermochronology of the Pan-African Damara Orogeny, Namibia, with implications for tectonothermal and geodynamic evolution. Precambrian Research 150, 49-72

Hamilton, M.A., Sadowski, G.R., Teixeira, W., Ernst, R.E., and Ruiz, A.S. 2012. Precise, matching U-Pb ages for the Rincon del Tigre mafic layered intrusion and Huanchaca gabbro sill, Bolivia: Evidence for a late Mesoproterozic LIP in SW Amazonia? GAC-MAC Joint Annual Meeting, St. John's 2012 Geoscience at the Edge, volume 35

Hamilton, M.A., and Buchan, K.L. U-Pb (2010). U-Pb geochronology of the Western Channel Diabase, northwestern Laurentia: Implications for a large 1.59 Ga magmatic province, Laurentia's APWP and paleocontinental reconstructions of Laurentia, Baltica and Gawler craton of southern Australia. Precambrian Research 183, 463-473.

Hanson, R.E., Crowley, J.L., Bowring, S.A., Ramezani, J., Gose, W.A., Dalziel, I.W.D, Pancake J.A., Seidel, E.K., Blenkinsop, T.G., Mukwakwami, J., 2004. Coeval large-scale magmatism in the Kalahari and Laurentian cratons during Rodinia assembly. Science 304, 1126-1129.

Hanson, R.E., Harmer, R.E., Blenkinsop, T.G., Buller, D.S., Dalziel, I.W.D., Gose, W.A., Hall, R.P., Kampunzu, A.B., Key, R.M., Mukwakwami, J., Munyanyiwa, H., Pancake, J.A., Seidel, E.K., Ward, E.K., 2006. Mesoproterozoic intraplate magmatism in the Kalahari craton: a review. Journal of African Earth Sciences 46, 141-167.

Hanson, R.E., Martin, M.W., Bowring, S.A., Munyanyiwa, H., 1998. U-Pb zircon age for the Umkondo dolerites, eastern Zimbabwe: 1.1 Ga large igneous province in southern Africa – East Antarctica and possible Rodinia correlations. Geology 26, 1143-1146.

Heaman, L., 1991. U/Pb dating of giant radiating dyke swarms: Potential for global correlation of mafic magmatic events. In: International Symposium of mafic dykes. Extended abstracts, São Paulo, Brazil, p. 7-9.

Heaman, L.M., Easton, R.M., Hart, T.R., Hollings, P., MacDonald, C.A., Smyk, M., 2007. Further refinement of the timing of Mesoproterozoic magmatism, Lake Nipigon region, Ontario. Canadian Journal of Earth Sciences 44, 1055-1086, doi: 10.1139/E06-117.

Irvine, T.N., Barager, W.R., 1971. A guide to the chemical classification of the common volcanic rocks. Canadian Journal of Earth Sciences 8, 523-548

Jaffey, A.H., Flynn, K.F., Glendenin, L.E., Bentley, W.C. and Essling, A.M. 1971. Precision measurement of half-lives and specific activities of 235U and 238U. Physical Review 4, 1889-1906.

Jacobs, J., Pisarevsky, S.A., Thomas, R.J., Becker T., 2008. The Kalahari Craton during the assembly and dispersal of Rodinia. Precambrian Research 160, 142-158. doi:10.1016/j.precamres.2007.04.022

Khudoley, A.K., Kropachev, A.P., Tkachenko, V.I., Rublev, A.G., Sergeev, S.A., Matukov, D.I., Lyahnitskaya, O.Yu., 2007. Mesoproteroic to Neoproterozoic Evolution of the Siberian craton and adjacent microcontinents: an overview with constraints for a Laurentian connection. Proterozoic Geology of Western North America and Siberia. SEPM Special Publication No. 86, p. 209–226.

Khudoley, A.K., Chamberlain, K.R., Schmitt, A.K., Harrison, T.M., Prokopiev, A.V., Sears, J.W., Veselovskiy, R.V., Proskurnin, V.F., 2009. New U-Pb baddeleyite ages from mafic intrusions from Taimyr, northern and southeastern Siberia: implications for tectonic and stratigraphy. In: Isotopic systems and the timing of geological processes. Materials of the IV Russian conference on isotopic geology. Vol. 2, Saint-Petersburg, pp. 243-245. [in Russian].

Kokonyagni, J.W., Kampunzu, A.B., Armstrong, R., Yoshida, M., Okudaira, T., Arima, M., Ngulube, D.A., 2006. The Mesoproterozoic Kibaride belt (Katanga, SE D.R. Congo). Journal of African Earth Sciences 46, 1-35.

Kröner, A., 1982. Rb/Sr geochronology and tectonic evolution of the Pan-African Damara Belt of Namibia, Southwestern Africa. American Journal of Science, Vol. 282, 1471-

1507.

Kröner, A., Cordani, U., 2003. African, southern India and South Américam cratons were not part of the Rodinia supercontinent: evidence from field relationships and geochronology. Tectonophysics 375, 325-352.

Li, Z.X., Bogdanova, S.V., Collins, A.S., Davidson, A., De Waele, B., Ernst, R.E., Fitzsimons, I.C.W., Fuck, R.A., Gladkochub, D.P., Jacobs, J., Karlstrom, K.E., Lul, S., Natapovm, L.M., Pease, V., Pisarevsky, S.A., Thrane, K. and Vernikovsky, V., 2008. Assembly, configuration, and break-up history of Rodinia: A synthesis. Precambrian Research 160, 179-210.

Loewy, S.L., Dalziel, I.W.D., Pisarevsky, S., Connely, J.N., Tait, J., Hanson, R.E., Bullen, D., 2011. Coats Land crustal block, East Antarctica: A tectonic tracer for Laurentia? Geology 39, 859-862, doi: 10.1130/G32029.1.

Ludwig, K.R., 2003. User's Manual for Isoplot 3.00 A Geochronological Toolkit for Excel. Berkeley Geochronological Center, Special Publication No. 4, p. 71.

Machado, M.J. Canto, Santos, R., 2006. Proficiency testing programs – a tool in the validation process of an analytical methodology for quantification of rare earth elements by ICP-MS. Spectra Analyse 252, 28-38.

Maier, W.D., 2008. The Kunene anorthosite Complex, its satellite intrusions, and possible links to early Kibaran intrusions in Tanzania and Burundi. October 2008 LIP of the Month. http://www.largeigneousprovinces.org/08oct.html

Maier, W.D., Peltonen, P., Livesey, T., 2007. The ages of the Kabanga North and Kapalagulu intrusions, Western Tanzania: a reconnaissance study. Economic Geology 102, 147-154.

Maier, W.D., Teigler, B., Miller, R., 2008. The Kunene anorthosite complex and its satellite intrusions. In R.Mc.G. Miller, (ed.), The Geology of Namibia, Geological Survey of Namibia, 9-1 to 9-18.

Martin, H., 1983. Overview of thegeosynclinal,structural and metamorphic development of the intracontinental branch of the Damara orogen. In: Martin, H., Eder, F.W. (Eds.), Intracontinental Fold Belts. Springer-Verlag, Berlin, 473-502.

Mayer, A., Hofmann, A.W., Sinigoi, S., Morais, E., 2004. Mesoproterozoic Sm-Nd and U-Pb ages for the Kunene Anorthosite Complex of SW Angola. Precambrian Research 133, 187-206

McCourt, S., Armstrong, R.A., Kampunzu, A.B., Mapeo, R.B. and Morais, E., 2004. New U-Pb SHRIMP ages on zircons from the Lubango region, Southwest Angola: insights into the Proterozoic evolution of South-Western Africa. (Abstract) *Geoscience Africa 2004*. (Symposium: The birth and grouth of continents – Geodynamics through time)

Meert, J.G. 2012. What's in a name? The Columbia (Paleopangaea/Nuna) supercontinent, Gondwana Research 21 (2012) 987–993, doi:10.1016/j.gr.2011.12.002.

Menge, G.F.W., 1998. The antiformal structure and general aspects of the Kunene Complex, Namibia. Z. Dt. Geol. Ges. 149/3, 431-448.

Meschede, M., 1986. A method of discriminating between different types of mid-ocean ridge basalts and continental tholeiites with Nb-Zr-Y diagram. Chemical Geology 56, 207-218.

Miller, R. McG., 1983. The Pan-African Damara orogen of South West Africa/Namibia. In: Miller, R. McG. (Ed.), Evolution of the Damara Orogen of South West Africa/Namibia. Special Publication Geological Society of South Africa, 11, 431-515.

Morais, E., Sinigoi, S., Mayer, A., Mucana, A., Rufino Neto, J., 1998. The Kunene gabbro-anorthosite complex: preliminary results based on new field and chemical data. African Geoscience Review 5, 485-498.

Nakamura, N., 1974. Determination of REE, Ba, Fe, Mg, Na and K in carbonaceous and ordinary condrites. Geochimica et Cosmochimica Acta 38, 757-775

Okrugin, A.V., Oleinikov, B.V., Savvinov, V.T., Tomshin, M.D., 1990. Late Precambrian dyke swarms of the Anabar Massif, Siberian Platform, USSR. In: Parker, A.J., Rickwood, P.C., Tucker, D.H. (eds.) Mafic Dykes and Emplacement Mechanisms. Balkema, Rotterdam, p. 529-533.

Passchier, C.W., Trouw, R.A.J., Ribeiro, A., Paciullo, F.V.P., 2002. Tectonic evolution of the southern Kaoko Belt, Namibia. Journal of African Earth Sciences 35, 61-75

Pearce, J.A., Norry, M.J., 1979. Petrogenetic Implications of Ti, Zr. and Nb variations in volcanic rocks. Contributions to Mineralogy and Petrology 69, 33-47

Pereira, E., 1973. Carta Geológica de Angola na escala 1/100.000. Notícia Explicativa da Folha 335 (Vila Arriaga). Rel. Inédito Serviço de Geologia e Minas de Angola Luanda.

Pereira, E., Moreira, A., 1978 - Sobre o complexo de estruturas anelares da Serra da Neve (Angola). II Centenário Academia das Ciências, Lisboa. Estudos de Geologia, Paleontologia e Micologia, 97-120

Pereira, E., Moreira, A., Van Dunen, M.V., Gonçalves, F.G., 2001 – Carta Geológica de Angola à escala 1: 250 000. Notícia Explicativa da Folha Sul D-33 / H (Chongoroi). Publicação do Instituto Geológico de Angola, 46 pp.

Pereira, E., Van-Dúnen, M. V., Tassinari, C.C.G., 2006. Carta Geológica de Angola à escala 1: 100 000. Notícia Explicativa da Folha Sul D-33/N-III (Bibala). Instituto Geológico de Angola, 57 pp.

Pereira, E., Tassinari, C.G., Rodrigues, J.F., Van-Dúnen, M.V., 2011. New data on the deposition age of the volcano-sedimentary Chela Group and its Eburnean basement: implications to post-Eburnean crustal evolution of the SW of Angola. Comunicações Geológicas do LNEG 98, 29-40

Pimentel, M.M., Fuck, R.A., Jost, H., Ferreira Filho, C.F., Araújo, S.M., 2000. The basement of the Brasília Fold Belt and the Goiás Magmatic Arc. In: Cordani, U.G., Milani, E.J., Thomaz Filho, A., Campos, D.A. (Eds.), Proceedings of the 31st International Geological Congress on The Tectonic Evolution of South America. Rio de Janeiro, pp. 195–229.

Pimentel, M., Fuck, R.A., 1992. Neoproterozoic crustal accretion in Central Brazil. Geology 20 (4), 375–379.

Piper, J.D.A., 1974. Magnetic properties of the Cunene Anorthosite Complex, Angola. Physics of the Earth and Planetary Interiors 9, 353-363.

Pisarevsky, S.A., Natapov, L.M., 2003. Siberia and Rodinia. Tectonophysics 375, 221-245.

Pisarevsky, S.A., Wingate, M.T.D., Powell, C.McA., Johnson, S., Evans, D.A.D., 2003. Models of Rodinia assembly and fragmentation. In: Yoshida, M., Windley, B., Dasgupta, S. (eds). Proterozoic East Gondwana: supercontinent assembly and breakup. Geological Society of London Special Publication 206, 35-55.

Pisarevsky, S.A., Natapov, L.M, Donskaya, T.V., Gladkochub, D.P., Vernikovsky, V.A., 2008. Proterozoic Siberia: A promontory of Rodinia. Precambrian Research 160, 66-76.

Pisarevsky, S.A., Bylund, G., 2010. Paleomagnetism of 1780-1770 Ma mafic and composite intrusions of Småland (Sweden): implications for the Mesoproterozoic supercontinent. American Journal of Science 310, 1168-1186.

Powell, C.McA, Jones, D.L, Pisarevsky, S.A., Wingate, M.T.D., 2001. Paleomagnetic constraints on the position of the Kalahari craton in Rodinia. Precambrian Research 110, 33-46.

Prave, A.R., 1996. Tale of three cratons: tectonostratigraphic anatomy of the Damara orogen in northwestern Namibia and the assembly of Gondwana. Geology 24, (12), 1115-1118.

Puchkov, V.N., Bogdanova, S.V., Ernst, R.E., Kozlov, V.I., Krasnobaev, A.A., Söderlund, U., Wingate, M.T.D., Postnikov, A., Sergeeva, N.D., 2012. New U-Pb geochronology of the ca. 1380 Ma Mashak igneous event of the Southern Urals and adjacent area: implications for Mesoproterozoic breakup of the eastern margin of the East European craton. Lithos (Special Issue), submitted

Pradhan, V.R., Meert, J.G., Pandit, M.K., Kamenov, G., Mondal, Md.E.A., 2012. Paleomagnetic and geochronological studies of the mafic dyke swarms of Bundelkhand craton, central India: Implications for the tectonic evolution and paleogeographic reconstructions. Precambrian Research 198-199, 51–76, doi:10.1016/j.precamres.2011.11.011

Rainbird, R.H., Stern, R.A., Khudoley, A.K., Kropachev, A.P., Heaman, L.M., Sukhorukov, V.I., 1998. U-Pb geochronology of Riphean sandstone and gabbro from southeast Siberia and its bearing on the Laurentia-Siberia connection. Earth and Planetary Science Letters 164, 409-420.

Renne, P.R., Onstott, T.C., D’Agrella-Filho, M.S., Pacca, I.G., and Teixeira, W., 1990, $^{40}Ar/^{39}Ar$ dating of 1.0–1.1 Ga magnetizations from the São Francisco and Kalahari cratons: Tectonic implications for Pan-African and Brasiliano mobile belts: Earth and Planetary Science Letters, v. 101, p. 349–366.

Seth, B., Armstrong, R.A., Sönke Brandt, Villa, I.M., Kramers, J.D., 2003. Mesoproterozóic U-Pb and Pb-Pb ages of granulites in NW Namibia: reconstructing a complete orogenic cycle. Precambrian Research 126, 147-168

Seth, B., Kröner, A., Mezger, K, Nemchin, A., Pidgeon, R.T., Okrusch, M., 1998. Archean to Neoproterozoic magmatic events in the Kaoko belt of NW Namibia and their geodynamic significance. Precambrian Research 92, 341-363.

Silva, A.T.F., 1980. Idade radiométrica K/Ar do dique norítico de Vila Arriaga e sua relação com a do Grupo Chela (Angola). Memórias da Academia das Ciências, Lisboa 21, 137-159

Silva, A.T.F., Torquato, J.R., Kawashita, K., 1973 – Alguns dados geocronológicos pelo método K/Ar da região de Vila Paiva Couceiro, Quilengues e Chicomba (Angola). Serviço de Geologia e Minas de Angola, Boletim 24, 29-46.

Silva, L.C., 1972. O maciço gabro-anortosítico do SW de Angola. Revista da Faculdade de Ciências, Universidade de Lisboa, 2 sér. Vol. XVII, Fasc. 1, pp. 253-277

Silva, Z.C.G., 1990. Geochemistry of the Gabbro-Anorthosite Complex of Southwest Angola. Journal of African Earth Sciences 10, 683-692

Silva, Z.C.G., 1992. Mineralogy and cryptic layering of the Kunene anorthosite complex of SW Angola and Namibia. Mineralogical Magazine 56, 319-327.

Silveira, E.M., Söderlund, U., Oliveira, E.P., Ernst, R.E., Menezes Leal, A.B., 2012 First precise U-Pb baddeleyite ages of 1500 Ma mafic dykes from the São Francisco Craton, Brazil, and tectonic implications. Lithos (Special Issue), in press

Simões, M.C., 1971. Contribuição para o conhecimento petrológico de alguns filões noríticos do Sudoeste de Angola. Serviço de Geologia e Minas de Angola, Boletim 23, 21-40

Simpson, E.S.W. and Otto, J.D.T., 1960. On the Precambrian anorthosite mass of southern Angola. 21st Internation Geological Congress Copenhagen, 13, 216-227.

Sleijko, F., Demarchi, G., Morais, E., 2002. Mineral chemistry and Nd isotopic composition of two anorthositic rocks from the Kunene Complex (South Western Angola). Journal of African Earth Sciences 35, 77-88.

Stone, P. and Brown, G.M., 1958. The Quihita-Cunene layered gabbroic intrusion of south-west Angola. Geological Magazine 95, 195-204

Sun, S., McDonough, W.F., 1989. Chemical and isotopic systematics of ocean basalts: implications for mantle composition and processes. In: Saunders, A.D.N., Norry, M.J. (Eds.), Magmatism in the Ocean Basins. Geological Society of London Special Publication, 313–345.

Tack, L., Wingate, M.T.D. De Waele, B, Meert, J., Belousova, E., Griffin, B., Tahon, A., Fernandez-Alonso, M., 2010. The 1375Ma “Kibaran event” in Central Africa: Prominent emplacement of bimodal magmatism under extensional regime. Precambrian Research 180, 63–84, doi:10.1016/j.precamres.2010.02.022

Taylor, S.R., McLennan, S.M., 1985. The continental crust: its composition and evolution. Oxford, Blackwell. 328 pp.

Torquato, R. e Amaral, G., 1973. Idade K/Ar em rochas de Catanda e Vila de Almoster. Instituto de Investigação Científica de Angola, Boletim 10 (1). 89-95, Luanda.

Trompette, R., 1994. Geology of Western Gondwana (2000 - 500 Ma). A.A. Balkema, Rotterdam/Brookfield, 350 p.

Upton, B.G.J., Rämö, O.T., Heaman, L.M., Blichert-Toft, J., Kalsbeek, F., Barry, T.L., and Jepsen, H.F. 2005. The Mesoproterozoic Zig-Zag Dal basalts and associated intrusions of eastern North Greenland: mantle plume-lithosphere interaction. Contributions to Mineralogy and Petrology, 149, 40-56.

Vale, F.S., Simões, M.C., 1971. Carta Geológica de Angola à escala 1: 100 000. Notícia Explicativa da Folha 336 (Sá da Bandeira). Serviço de Geologia e Minas de Angola, 36 pp.

Vale, F.S., Simões, M.C., 1973. Carta Geológica de Angola à escala 1: 100 000. Notícia Explicativa da Folha 356 (Vila João de Almeida). Serviço de Geologia e Minas de Angola, 42 pp.

Vale, F.S., Cruz, A.G., Pereira, E., Simões, M.C., 1972 - Carta Geológica de Angola na escala 1/100.000. Notícia Explicativa da Folha 316 (Dinde-Lola). Serviço de Geologia e Minas, Angola, 40 pp.

Vale, F.S., Gonçalves, F.G., Simões, M.C., 1973. Carta Geológica de Angola à escala 1: 100 000. Notícia Explicativa da Folha 355 (Humpata-Cainde). Serviço de Geologia e Minas de Angola, 38 pp.

Vernikovsky, V.A., 1996. Geodynamic evolution of Taimyr folded area. Siberian Branch RAS SPC UIGGM, 202 pp. (in Russian).

Vernikovsky, V.A., Vernikovskaya, A.E., 2001. Central Taimyr accretionary belt (Arctic Asia): Meso–Neoproterozoic tectonic evolution and Rodinia breakup. Precambrian Research 110, 127–141.

Veselovskiy, R. V., Petrov, P. Yu., Karpenko, S. F., Kostitsyn, Yu. A., Pavlov, V. E., 2006. New Paleomagnetic and Isotopic Data on the Mesoproterozoic Igneous Complex on the Northern Slope of the Anabar Massif. Transactions (Doklady) of the Russian Academy of Sciences, Earth Science Section 411(8), 1190-1194.

Winchester, J.A., Floyd, P.A., 1977. Geochemical discriminanation of different magma series and their differentiation product using immobile elements. Chemical Geology 20, 325-343

Wingate, M.T.D., Pirajno, F., Morris, P.A. 2004. Warakurna large igneous province: A new Mesoproterozoic large igneous province in west-central Australia. Geology 32(2), 105-108.

Wingate, M.T.D., Pisarevsky, S.A., Gladkochub, D.P., Donskaya, T.V., Konstantinov, K.M., Mazukabzov, A.M., Stanevich, A.M., 2009. Geochronology and paleomagnetism of mafic igneous rocks in the Olenek Uplift, northern Siberia: implications for Mesoproterozoic supercontinents and paleogeography. Precambrian Research 170, 256-266.

FIGURE CAPTIONS

Figure 1*. Generalized geology of southern Africa and the São Francisco craton of South America attached in the Gondwana/Pangea reconstruction. The generalized distribution of proposed LIP events is shown, and discussed in the text. Red corresponds to 1500 Ma event, green to the 1380 Ma event and blue to the 1110 Ma event. The heavy dashed line marks the possible boundary of the Congo craton at 1.0 Ga. KAB = Karagwe-Ankole belt and KIB = Kibara belt, as defined by Tack et al. (2010). They contain bimodal magmatism of 1375 Ma age including in the Kabanga-Musongat-Kapalagulu mafic-ultramafic complex and S-type granites. The outline of Angola is also shown.*

Figure 2. *LIP barcode comparison of the crustal blocks discussed in this paper. Data is mainly from Ernst et al. (2008), with the exception of 1500 Ma ages for the São Francisco craton from Silveira et al. (2012), the 1110 Ma ages for Amazonia from Hamilton et al. (2012), the 1110 Ma age for Greater India from Pradhan et al. (2012) and the KAB and KIB ages from Congo (Tack et al. 2010). Events labelled in UPPER CASE are true LIPs in terms of size, duration and intraplate setting (per the criteria of Bryan and Ernst, 2008) while others are interpreted as remnants of LIPs (after erosion and continental breakup). The two new U-Pb baddeleyite ages reported herein are each enclosed by a rectangle.*

Figure 3. *Geology of the Bibala-Lubango-Cainde region of Angola in the southwestern branch of the Congo craton. A) Geology, B) Dyke Swarms, and sample sites, located by black circles. Faults not shown. Sample site labels correspond to the portion of the full sample number after the dash. For instance, the site for sample "356-17" is labelled as "17". Coordinates of samples sites are given in Table 2.*

Figure 4 *- Diagrams for dolerite sills intrusive into the Chela Group: a) Log (Zr/TiO2)–log (Nb/Y) classification diagram (Winchester and Floyd, 1977); b) Zr/Y-Zr (Pearce and Norry, 1979); c) Zr/4-Y-Nb*2 diagram (Meschede, 1986); d) primordial mantle-normalised multi-element spider diagrams (values of Sun and McDonough, 1989); e) chondrite-normalized rare-earth-element (REE) patterns. Colour-coding is explained in Table 3.*

Table 1. Intraplate magmatic barcode record of the São Francisco – Congo craton

1110 Ma	**Location**	**Composition**	**U-Pb (z= zircon, b = baddeleyite)**	**Reference**
Gabbro Norite dykes (NNW-NNE trending)	SW Angola (Congo craton)	Norite	1110 ± 3 Ma (b)	herein
1380 Ma				
KIC (Kunene instrusive complex): includes GC (gabbro-anorthosite complex) and anorthosite complex of Zebra mountains	Angola/Namibia (Congo craton)	Gabbro-Anorthosite complex	1385 ± 25 (z) 1371 ± 3 Ma (z) 1385 ± 8 Ma (z)	Mayer et al. (2004) McCourt et al. (2004) Drüpel et al. (2007)
Red granites	Angola (Congo craton)	Silicic	1376 ± 2 Ma (z)	Drüpel et al. (2007)
KAB (Karagwe-Ankole belt) includes: Kabanga-Musongati-Kapalaglula (mafic ultramafic intrusions) and S-type granitods	Congo, Tanzania (Congo craton)	Bimodal intrusions	1370-1380 Ma (z)	Tack et al. (2010) and references therein
KIB (Kibara belt),	Congo, Tanzania (Congo craton)	Bimodal intrusions	1370-1380 Ma (z)	Tack et al. (2010) and references therein
1500 Ma				
Humpata and related sills	SW Angola (Congo craton)	Mafic	1502 ± 4 Ma (b)	herein
Curaçá and Chapada Diamantina dykes and sills	Brazil (Sao Francisco craton)	Mafic	1503-1508 Ma (b)	Silveira et al. (2012)

Table 2. Geographic coordinates of samples

Rock type	Sample	Coordinates		
		Latitude	Longitude	
Sills	335-4	14 55´ 01´´S	13 15´15´´ E	
	356-56	15 13´51´´S	13 30´33´´E	
	355-57	15 08´17´´ S	13 19´18´´E	
	355-58	15 15´03´´ S	13 24´52´´ E	
Diabase	335-10	14 42´06´´S	13 19´30´´ E	
Subophitic gabbro	335-14a	14 39´02´´S	13 23´55´´E	
Gabbro-norites	335-6a	14 42´05´´S	13 21´34´´ E	
	356-06	15 58´33´´ S	13 35´20´´ E	
	356-07	15 14´08´´ S	13 33´33´´ E	
	356-8	15 15´11´´ S	13 33´26´´ E	
	356-17	15 15´47´´ S	13 33´32´´ E	
	376-01	15 30´59´´ S	13 20´21´´ E	
	376-03	15 31´40´´ S	13 18´45´´E	
	377-53	15 49´09´´ S	13 38´33´´ E	

Table 3 - Chemical analysis of olivine dolerites

	SILLS				Olivine dolerites	
XFR	**335-4**	**356-56**	**355-57**	**355-58**	**335-10**	**335-14a**
Symbols		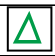				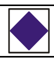
Major elements (%)						
SiO_2	45.50	42.66	53.64	53.79	51.07	51.92
Al_2O_3	13.96	15.44	13.48	13.59	12.49	12.45
Fe total (Fe_2O_3)	14.94	15.21	12.76	12.58	12.27	11.72
MnO	0.20	0.19	0.16	0.16	0.19	0.17
CaO	8.06	8.63	6.51	6.38	9.34	8.58
MgO	8.96	7.85	4.73	4.73	9.14	9.55
Na_2O	1.54	1.97	2.50	2.47	1.60	1.65
K_2O	1.40	0.90	1.80	1.86	0.90	1.07
TiO_2	1.54	2.74	1.64	1.59	0.84	0.90
P_2O_5	0.21	0.51	0.21	0.21	0.09	0.10
LOI	3.53	3.80	2.36	2.36	1.87	1.69
Sum	**99.84**	**99.90**	**99.79**	**99.72**	**99.80**	**99.80**
Trace elements (ppm)						
Rb	39	15	46	48	40	48
Sr	266	432	130	131	120	161
Y	21	29	34	33	17	19
Zr	98	136	193	194	77	89
Ba	303	466	389	410	187	224
Ni	183	215	111	95	196	239
Cu	71	44	105	102	101	96
Zn	107	110	108	107	81	96
Pb	6	6	16	15	9	13
Sc	29	22	23	26	34	30
V	219	221	217	209	225	207
Cr	160	97	232	217	634	642
Co	66	61	42	39	53	50
Ga	19	18	19	19	16	14
ICP-MS						
Nb	5.40	9.4	10.8	8.98	3*	4.29
Hf	2.56	3.3	4.50	3.33	<5*	1.13
Ta	0.68	0.61	0.65	0.53	<5*	0.15
Th	6.80	0.85	9.32	7.91	5*	3.90
U	2.48	0.17	2.57	2.24	<4*	1.05
La	14.0	17.2	32.1	26.8	11	14.6
Ce	32.1	39.9	57.1	49.9	24	24.6
Pr	4.0	5.7	7.19	6.28	2.7	3.19
Nd	18.0	26.3	29.0	26.4	12	13.6
Sm	3.9	5.9	6.64	5.90	2.6	3.17
Eu	1.5	2.0	1.75	1.56	0.9	0.91
Gd	4.4	6.2	7.27	6.54	3.2	3.72
Tb	0.7	0.90	1.13	1.04	0.5	0.62
Dy	4.4	5.5	7.06	6.21	3.5	3.83
Ho	0.9	1.1	1.41	1.26	0.7	0.78
Er	2.5	2.9	3.97	3.48	2.1	2.18
Tm	0.3	0.40	0.53	0.50	<0.4	0.31
Yb	2.3	2.5	3.61	3.19	1.9	2.05
Lu	0.3	0.35	0.52	0.48	0.3	0.31

(*) XRFanalysis

Sample nos.	**335-4**	**356-56**	**355-57**	**355-58**	**335-10**	**335-14a**
Symbols						
SmN	19.2	29.1	28.9	29.1	12.8	15.6
GdN	15.9	22.5	26.3	23.7	11.6	13.4
Eu/Eu*	0.8	1.01	0.8	0.77	1.04	0.82
LaN	42.4	52.1	97.3	81.2	33.3	44.2
YbN	10.4	11.4	16.4	14.5	8.6	9.3
LaN/YbN	4.1	4.6	5.9	5.6	3.9	4.8
Th/Nb	1.26	0.1	0.86	0.88	1.6	0.91
La/Nb	2.6	1.8	2.9	2.9	3.6	3.4
Zr/Nb	18.1	14.5	17.9	21.6	25.6	20.7
Hf/Th	0.38	3.8	0.48	0.42	1.0	0.29

Table 4 - Chemical analysis of gabbro-norites (GN)

Sample nos.	335-6A	356-06	356-07	356-8	356-17	376-01	376-03	377-53
Symbols								
Major elements (%)								
SiO_2	51.84	49.10	43.54	44.33	53.85	53.99	52.05	47.45
Al_2O_3	12.37	13.56	16.50	16.66	11.61	13.36	12.55	16.76
Fe total (Fe_2O_3)	11.76	16.13	14.08	13.79	10.61	9.69	11.62	14.12
MnO	0.18	0.24	0.17	0.18	0.16	0.15	0.17	0.18
CaO	8.54	8.54	9.61	8.98	6.33	8.56	8.79	8.41
MgO	9.47	5.12	6.69	6.52	11.4	8.24	9.16	6.73
Na_2O	1.71	2.45	1.69	1.97	1.72	1.72	1.70	2.25
K_2O	1.07	0.87	1.27	1.27	1.52	1.26	1.02	0.6
TiO_2	0.90	1.91	2.33	2.49	0.75	0.69	0.91	1.86
P_2O_5	0.10	0.25	0.44	0.42	0.08	0.08	0.10	0.24
LOI	1.83	1.62	3.53	3.17	1.88	1.97	1.63	1.24
Sum	**99.77**	**99.79**	**99.85**	**99.78**	**99.91**	**99.71**	**99.70**	**99.84**
Trace elements (ppm)								
Rb	49	38	23	25	61	52	43	25
Sr	157	280	383	377	161	150	135	325
Y	20	27	23	25	20	18	19	25
Zr	90	106	112	120	106	91	91	140
Ba	218	412	472	353	374	1244	217	216
Ni	252	56	119	131	362	141	218	158
Cu	101	65	103	42	84	76	95	80
Zn	96	117	95	97	76	68	81	110
Pb	15	9	<6	<6	11	9	11	7
Sc	32	39	21	22	26	30	30	27
V	202	328	229	194	183	164	204	212
Cr	642	93	68	108	999	399	576	127
Co	52	48	49	52	56	40	49	53
Ga	15	21	17	19	14	13	15	19
ICP-Ms								
Nb	5.10	3.82	9.51	8.2	5.2	6.15	7.67	7.6
Hf	1.60	2.41	2.08	2.8	2.1	2.56	2.63	4.0
Ta	0.30	0.10	0.41	0.56	0.38	0.28	0.42	0.61
Th	4.60	3.73	0.95	0.79	4.7	6.51	6.47	2.1
U	1.24	0.73	0.22	0.17	1.3	1.39	1.70	0.42
La	15.9	18.1	23.1	15.2	16.1	31.7	36.0	16.9
Ce	29.0	32.5	40.1	35.0	33.3	43.6	41.6	37.8
Pr	3.74	4.32	5.88	5.0	4.0	5.46	5.35	5.1
Nd	15.8	19.1	26.7	22.9	15.6	21.7	22.0	23.0
Sm	3.80	4.50	6.09	5.2	3.6	4.94	5.23	5.2

Eu	1.10	1.67	2.16	1.9	0.90	1.42	1.53	1.8
Gd	4.33	5.35	6.28	5.2	3.5	5.32	5.93	5.5
Tb	0.72	0.88	0.90	0.76	0.58	0.85	0.97	0.83
Dy	4.40	5.40	5.34	4.6	3.6	5.48	6.09	5.1
Ho	0.90	1.13	1.04	0.89	0.77	1.14	1.24	1.01
Er	2.56	3.20	2.90	2.5	2.4	3.33	3.49	2.8
Tm	0.37	0.45	0.36	0.31	0.29	0.46	0.49	0.41
Yb	2.39	3.02	2.44	2.1	2.0	3.20	3.32	2.5
Lu	0.36	0.44	0.35	0.28	0.25	0.47	0.49	0.37

Sample nos.	**335-6A**	**356-06**	**356-07**	**356-8**	**356-17**	**376-01**	**376-03**	**377-53**
EuN	14.3	21.7	28.0	24.7	11.7	18.4	19.8	23.4
SmN	18.7	22.2	30	25.6	17.7	24.3	25.8	25.6
GdN	15.7	19.4	22.8	18.8	12.7	19.3	21.5	19.9
Eu/Eu*	0.8	1.0	1.1	1.1	0.8	0.8	0.8	1.0
LaN	48.2	54.8	70	46.1	48.8	96.1	109.1	51.2
YbN	10.9	13.7	11.1	9.5	9.1	14.5	15.1	11.4
LaN/YbN	4.4	4.0	6.3	4.8	5.4	6.6	7.1	4.4
Th/Nb	0.9	1.0	0.1	0.1	0.9	1.1	0.8	0.3
Zr/Nba	17.6	27.7	11.8	14.6	20.4	14.8	11.9	18.4
Hf/Th	0.35	0.65	2.2	3.5	0.45	0.39	0.41	1.9

Table 5. Baddeleyite ID-TIMS U-Pb isotopic data for SW Angolan mafic magmatism, Congo Craton.

Fraction	Description	Weight (μg)	U (ppm)	Pb^T (pg)	Pb_C (pg)	Th/U	$^{206}Pb/^{204}Pb$	$^{206}Pb/^{238}U$	± 2σ	$^{207}Pb/^{235}U$	± 2σ	$^{207}Pb/^{206}Pb$	± 2σ	Ages (Ma) $^{206}Pb/^{238}U$	± 2σ	$^{207}Pb/^{235}U$	± 2σ	$^{207}Pb/^{206}Pb$	± 2σ	Disc. (%)
Sample **356-56**; Humpata olivine dolerite sill, intruding Chela Group																				
Bd-1	5 pale-med. brown blades	0.5	458	55.42	1.61	0.038	2349	0.254847	0.000557	3.29381	0.01265	0.093738	0.000261	1463.4	2.9	1479.6	3.0	1502.8	5.3	2.9
Bd-2	4 pale brown blades	0.1	101	24.14	1.65	0.038	1003	0.252324	0.000581	3.25630	0.02367	0.093598	0.000572	1450.4	3.0	1470.7	5.7	1500.0	11.6	3.7
Bd-3	4 pale brown blades	0.2	186	22.25	0.75	0.060	2013	0.251030	0.000566	3.23999	0.01380	0.093609	0.000293	1443.8	2.9	1466.8	3.3	1500.2	5.9	4.2
Sample **356-17**; subophitic, NNW-trending gabbro-norite dyke																				
Bd-1	5 pale-med brown blades	0.5	1258	67.16	1.11	0.133	4061	0.185456	0.000377	1.95668	0.00622	0.076520	0.000157	1096.7	2.0	1100.7	2.1	1108.7	4.1	1.2
Bd-2	5 pale brown blades	0.2	492	43.32	1.04	0.103	2833	0.184876	0.000373	1.95153	0.00741	0.076558	0.000217	1093.6	2.0	1099.0	2.5	1109.7	5.7	1.6
Bd-3	7 pale-med brown blades	0.4	1157	40.69	0.61	0.088	4515	0.185459	0.000361	1.95983	0.00580	0.076642	0.000147	1096.7	2.0	1101.8	2.0	1111.9	3.8	1.5

Notes:
All analyzed fractions represent best quality, fresh grains of baddeleyite.
Abbreviations: med - medium.
Pb^T is total amount (in picograms) of Pb.
Pb_C is total measured common Pb (in picograms) assuming the isotopic composition of laboratory blank: 206/204 - 18.221; 207/204 - 15.612; 208/204 - 39.360 (errors of 2%).
Pb/U atomic ratios are corrected for spike, fractionation, blank, and, where necessary, initial common Pb; 206Pb/204Pb is corrected for spike and fractionation.
Th/U is model value calculated from radiogenic 208Pb/206Pb ratio and 207Pb/206Pb age, assuming concordance.
Disc. (%) - per cent discordance for the given 207Pb/206Pb age.
Uranium decay constants are from Jaffey et al. (1971).

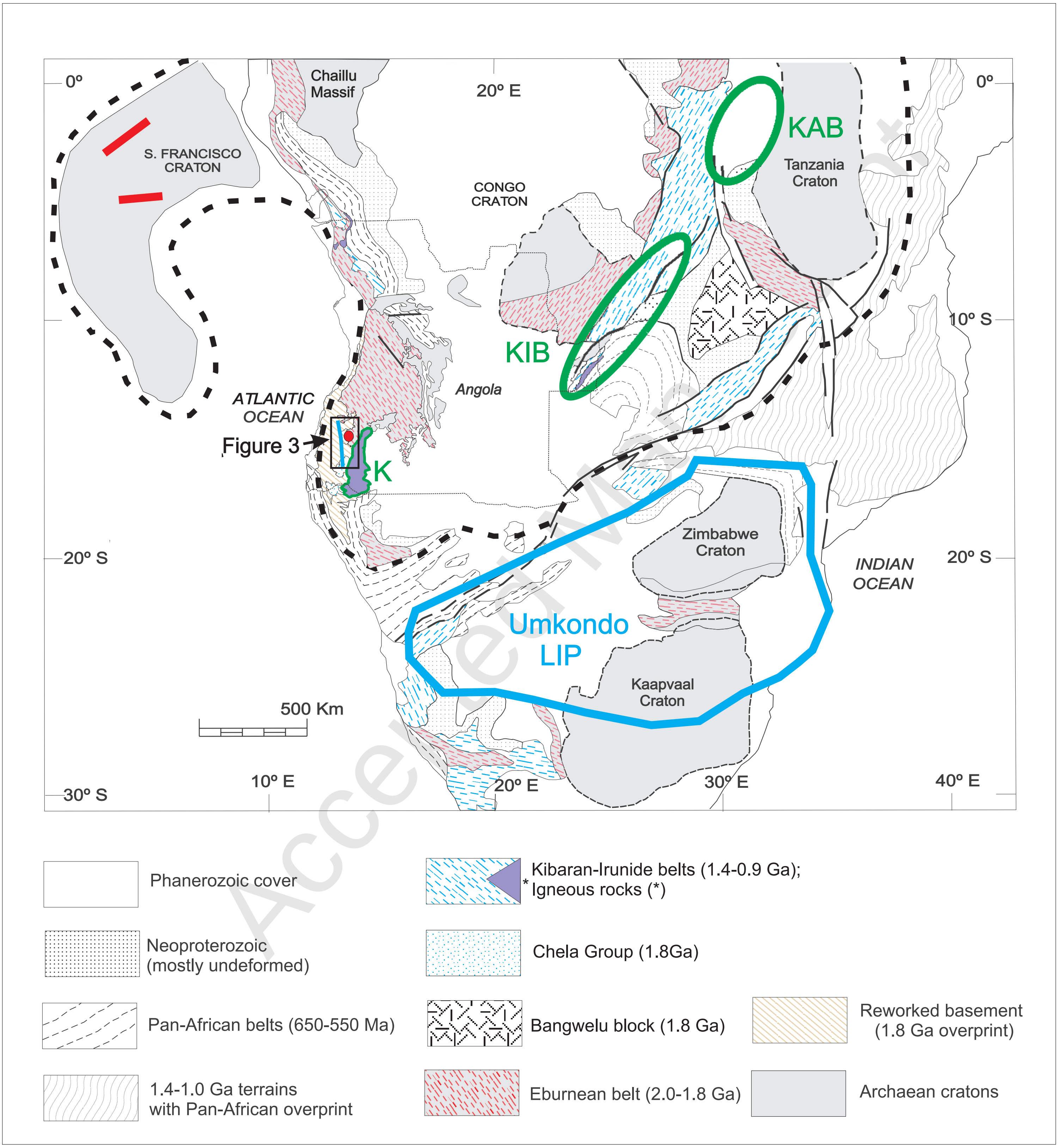
0°
Chaillu
Massif
20° E
0°
KAB
Tanzania
Craton
S. FRANCISCO
CRATON
CONGO
CRATON
10° S
KIB
Angola
ATLANTIC
OCEAN
Figure 3
K
Zimbabwe
Craton
20° S
INDIAN
OCEAN
20° S
Umkondo
LIP
Kaapvaal
Craton
500 Km
10° E
30° S
20° E
30° E
40° E
Phanerozoic cover
Kibaran-Irunide belts (1.4-0.9 Ga);
Igneous rocks (*)
Neoproterozoic
(mostly undeformed)
Chela Group (1.8Ga)
Pan-African belts (650-550 Ma)
Bangwelu block (1.8 Ga)
Reworked basement
(1.8 Ga overprint)
1.4-1.0 Ga terrains
with Pan-African overprint
Eburnean belt (2.0-1.8 Ga)
Archaean cratons

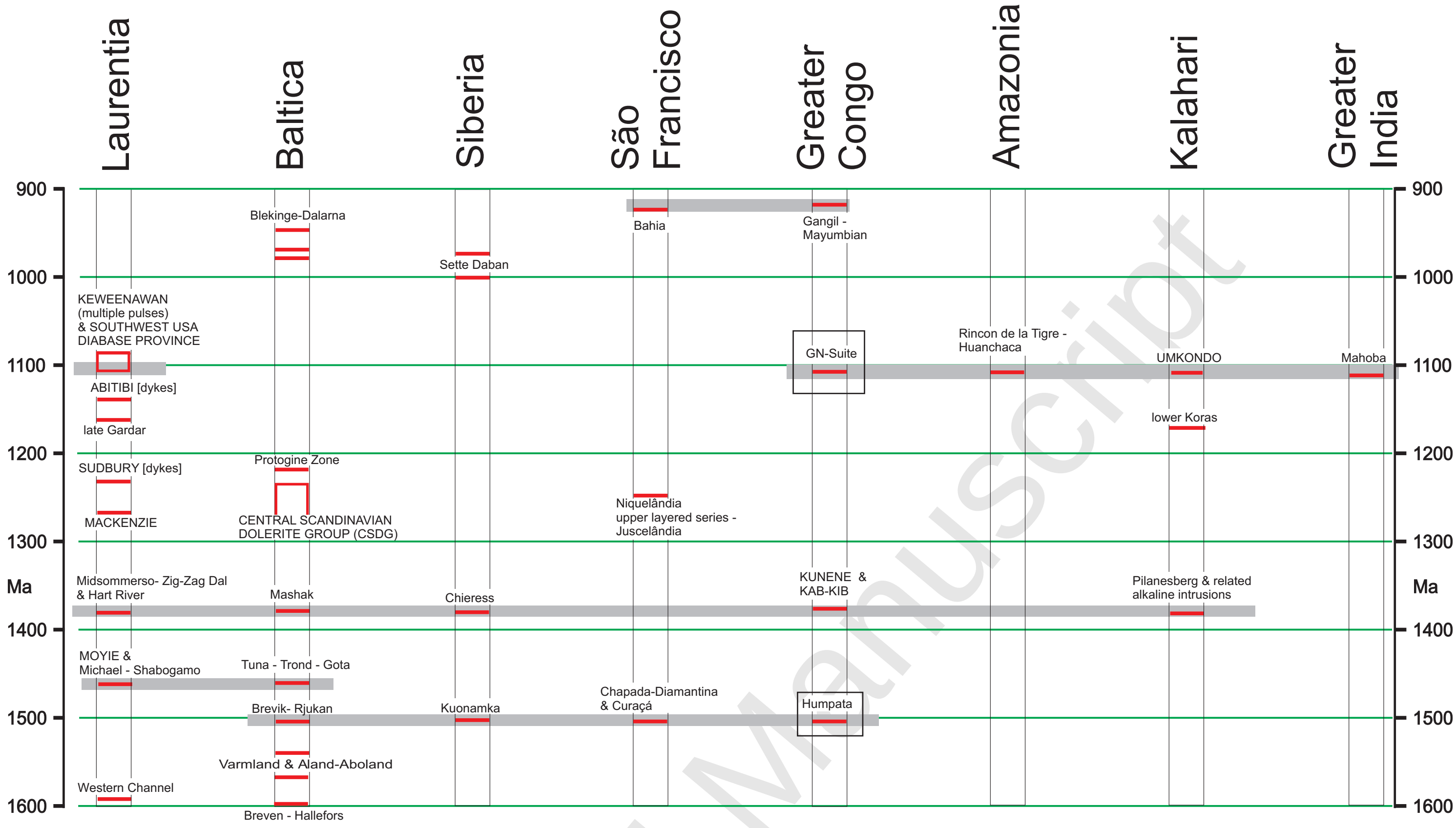

Laurentia
Baltica
Siberia
São Francisco
Greater Congo
Amazonia
Kalahari
Greater India
900
1000
1100
1200
1300
Ma
1400
1500
1600
Blekinge-Dalarna
Bahia
Gangil - Mayumbian
Sette Daban
KEWEENAWAN (multiple pulses) & SOUTHWEST USA DIABASE PROVINCE
GN-Suite
Rincon de la Tigre - Huanchaca
UMKONDO
Mahoba
ABITIBI [dykes]
lower Koras
late Gardar
Protogine Zone
SUDBURY [dykes]
Niquelândia upper layered series - Juscelândia
MACKENZIE
CENTRAL SCANDINAVIAN DOLERITE GROUP (CSDG)
Midsommerso- Zig-Zag Dal & Hart River
Mashak
Chieress
KUNENE & KAB-KIB
Pilanesberg & related alkaline intrusions
MOYIE & Michael - Shabogamo
Tuna - Trond - Gota
Chapada-Diamantina & Curaçá
Brevik- Rjukan
Kuonamka
Humpata
Varmland & Aland-Aboland
Western Channel
Breven - Hallefors

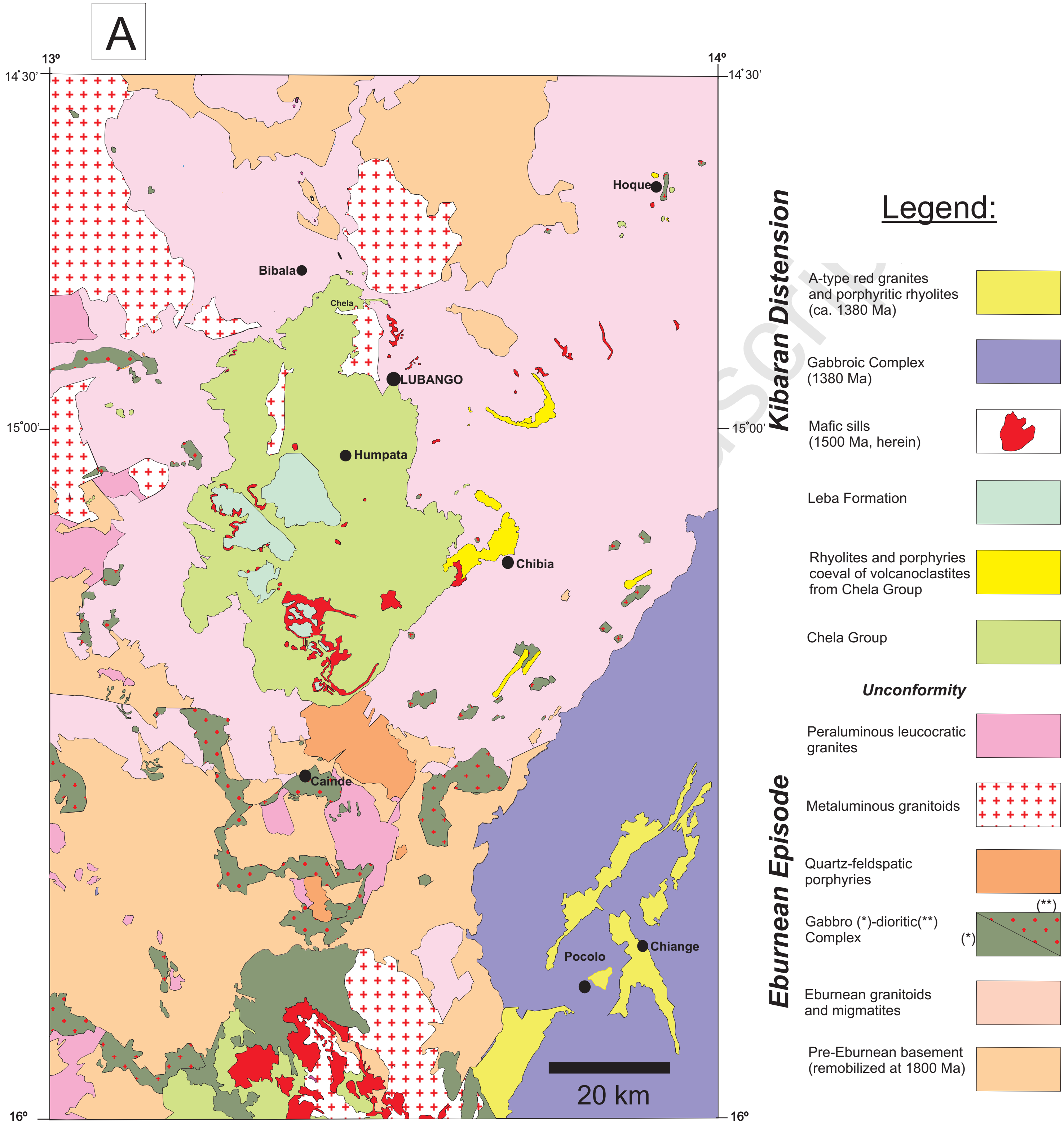
A
13º
14º
14˚30'
15˚00'
16º
Hoque
Bibala
Chela
LUBANGO
Humpata
Chibia
Cainde
Pocolo
Chiange
20 km
Legend:
Kibaran Distension
A-type red granites and porphyritic rhyolites (ca. 1380 Ma)
Gabbroic Complex (1380 Ma)
Mafic sills (1500 Ma, herein)
Leba Formation
Rhyolites and porphyries coeval of volcanoclastites from Chela Group
Chela Group
Unconformity
Eburnean Episode
Peraluminous leucocratic granites
Metaluminous granitoids
Quartz-feldspatic porphyries
Gabbro (*)-dioritic(**) Complex
(**)
(*)
Eburnean granitoids and migmatites
Pre-Eburnean basement (remobilized at 1800 Ma)

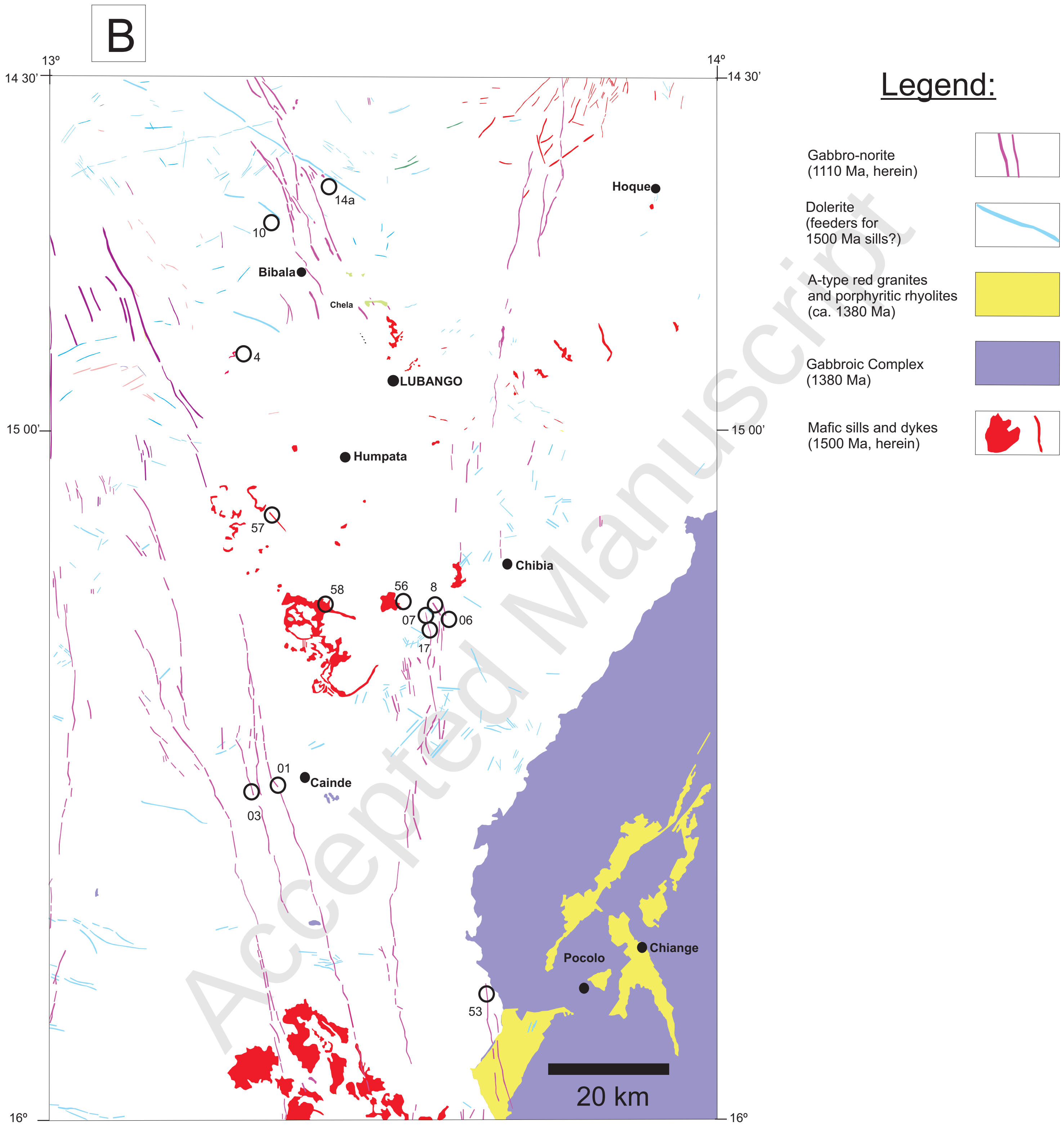
B
13º
14º
14 30'
14 30'
15 00'
15 00'
16º
16º
Hoque
14a
10
Bibala
Chela
4
LUBANGO
Humpata
57
Chibia
58
56
8
07
06
17
01
Cainde
03
Pocolo
Chiange
53
20 km
Legend:
Gabbro-norite
(1110 Ma, herein)
Dolerite
(feeders for
1500 Ma sills?)
A-type red granites
and porphyritic rhyolites
(ca. 1380 Ma)
Gabbroic Complex
(1380 Ma)
Mafic sills and dykes
(1500 Ma, herein)

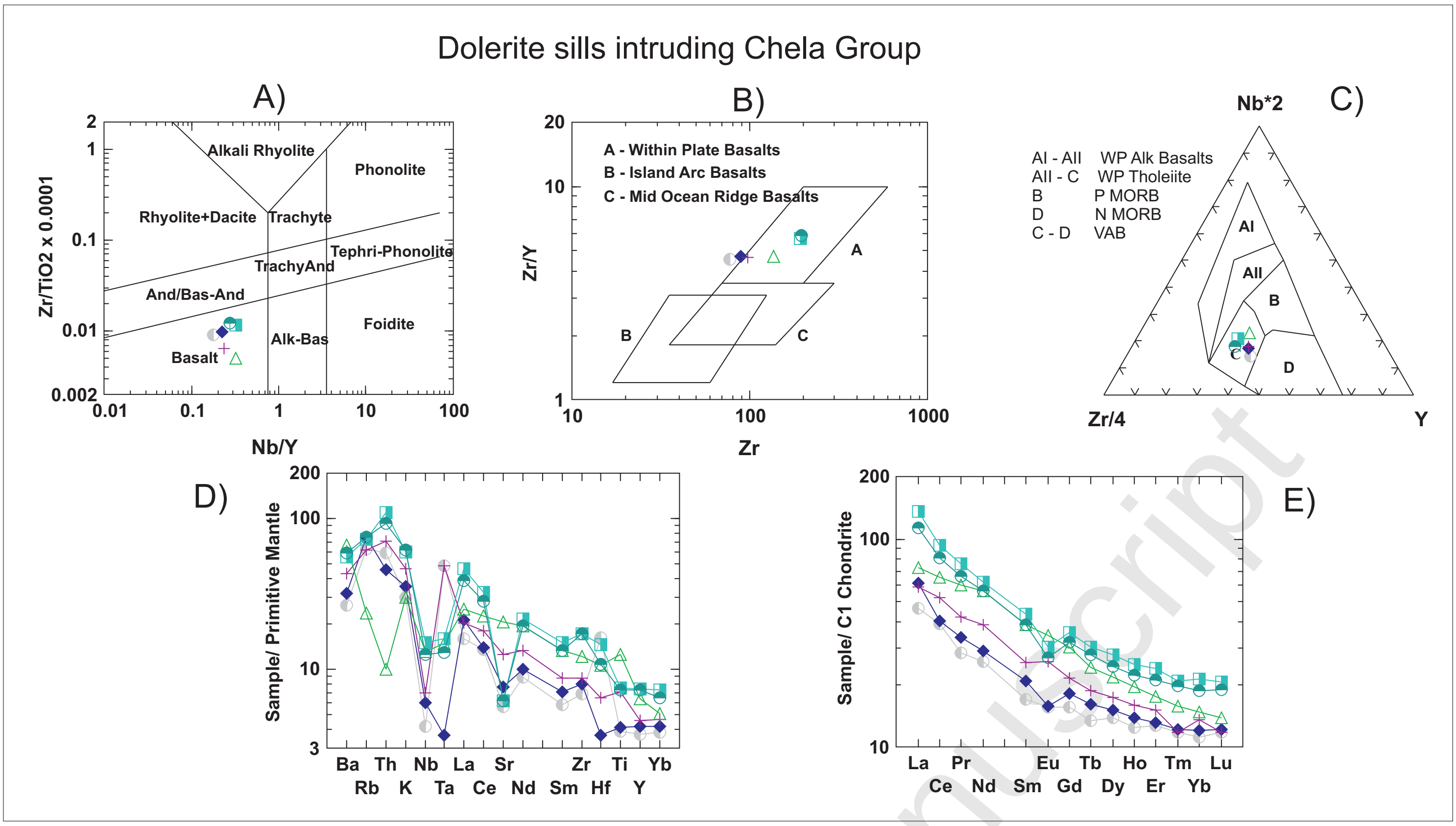
Dolerite sills intruding Chela Group
A)
Alkali Rhyolite
Phonolite
Rhyolite+Dacite
Trachyte
Tephri-Phonolite
TrachyAnd
And/Bas-And
Foidite
Alk-Bas
Basalt
Zr/TiO2 x 0.0001
Nb/Y
B)
A - Within Plate Basalts
B - Island Arc Basalts
C - Mid Ocean Ridge Basalts
Zr/Y
Zr
C)
Nb*2
AI - AII WP Alk Basalts
AII - C WP Tholeiite
B P MORB
D N MORB
C - D VAB
Zr/4
Y
D)
Sample/ Primitive Mantle
Ba Th Nb La Sr Zr Ti Yb
Rb K Ta Ce Nd Sm Hf Y
E)
Sample/ C1 Chondrite
La Pr Eu Tb Ho Tm Lu
Ce Nd Sm Gd Dy Er Yb

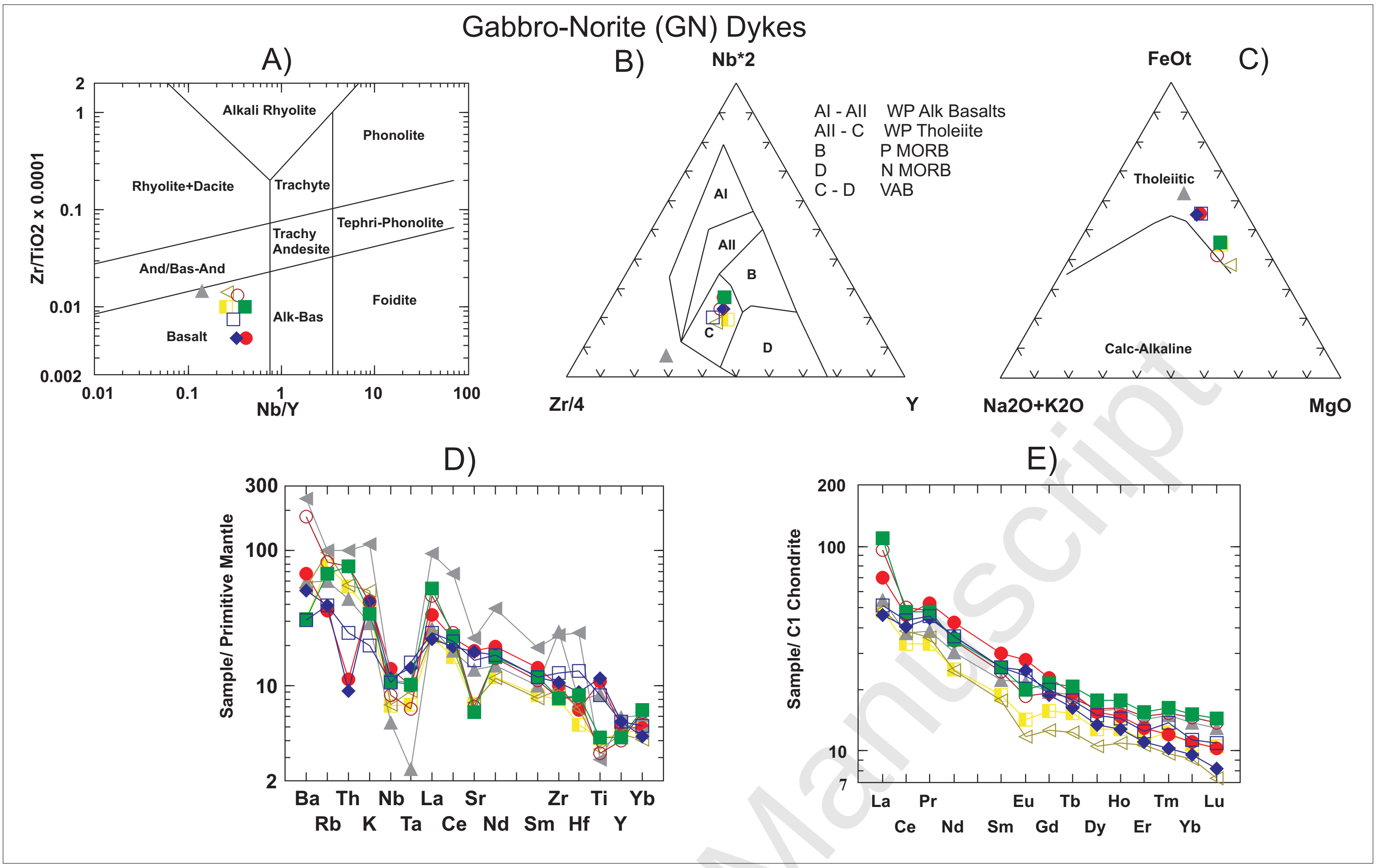
Gabbro-Norite (GN) Dykes
A)
Alkali Rhyolite
Phonolite
Rhyolite+Dacite
Trachyte
Tephri-Phonolite
Trachy Andesite
And/Bas-And
Foidite
Alk-Bas
Basalt
Zr/TiO2 x 0.0001
Nb/Y
B)
Nb*2
AI - AII WP Alk Basalts
AII - C WP Tholeiite
B P MORB
D N MORB
C - D VAB
AI
AII
B
C
D
Zr/4
Y
C)
FeOt
Tholeiitic
Calc-Alkaline
Na2O+K2O
MgO
D)
Sample/ Primitive Mantle
Ba Th Nb La Sr Zr Ti Yb
Rb K Ta Ce Nd Sm Hf Y
E)
Sample/ C1 Chondrite
La Pr Eu Tb Ho Tm Lu
Ce Nd Sm Gd Dy Er Yb

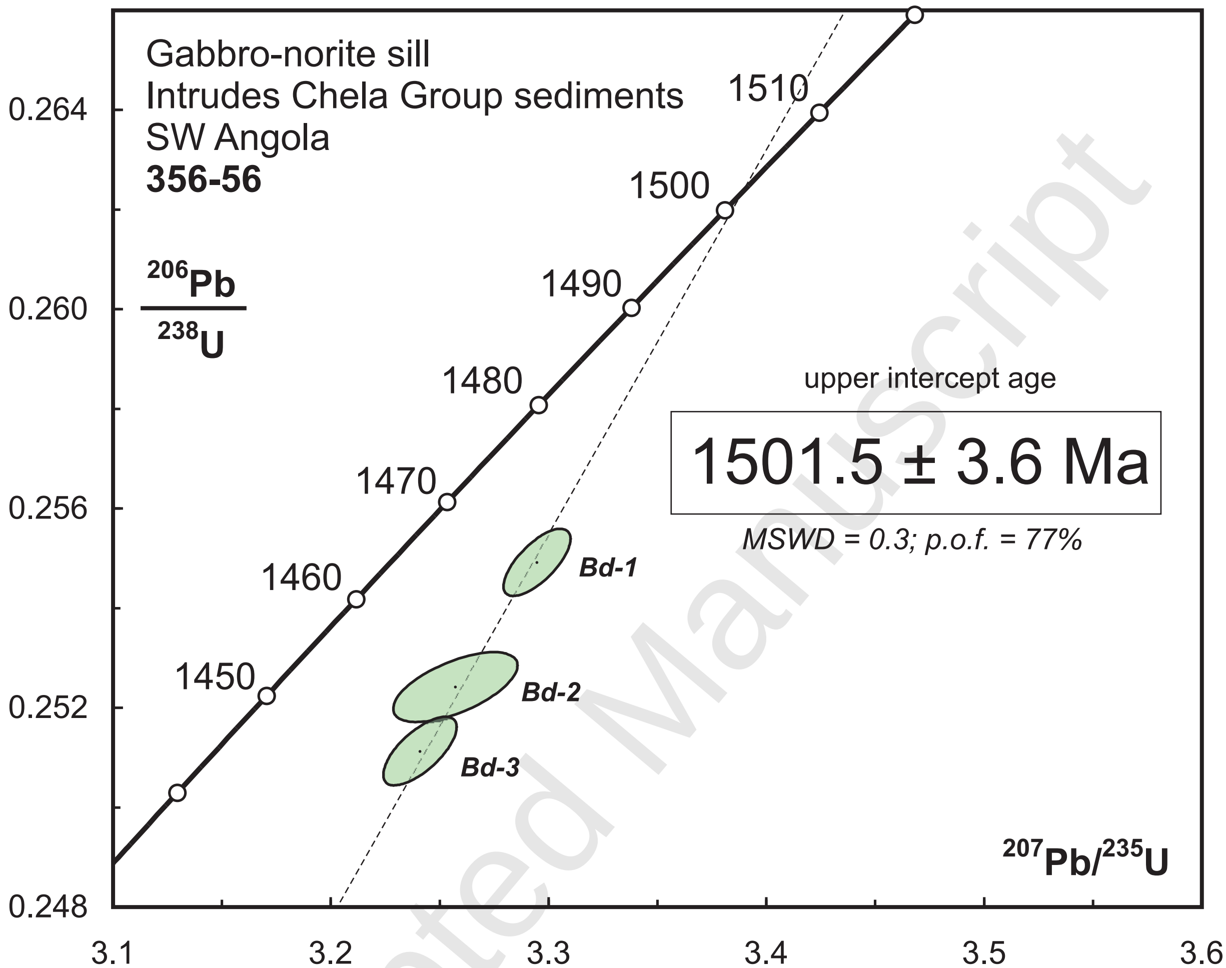
Gabbro-norite sill
Intrudes Chela Group sediments
SW Angola
356-56
206Pb/238U
207Pb/235U
upper intercept age
1501.5 ± 3.6 Ma
MSWD = 0.3; p.o.f. = 77%
Bd-1
Bd-2
Bd-3
1450
1460
1470
1480
1490
1500
1510
0.248
0.252
0.256
0.260
0.264
3.1
3.2
3.3
3.4
3.5
3.6

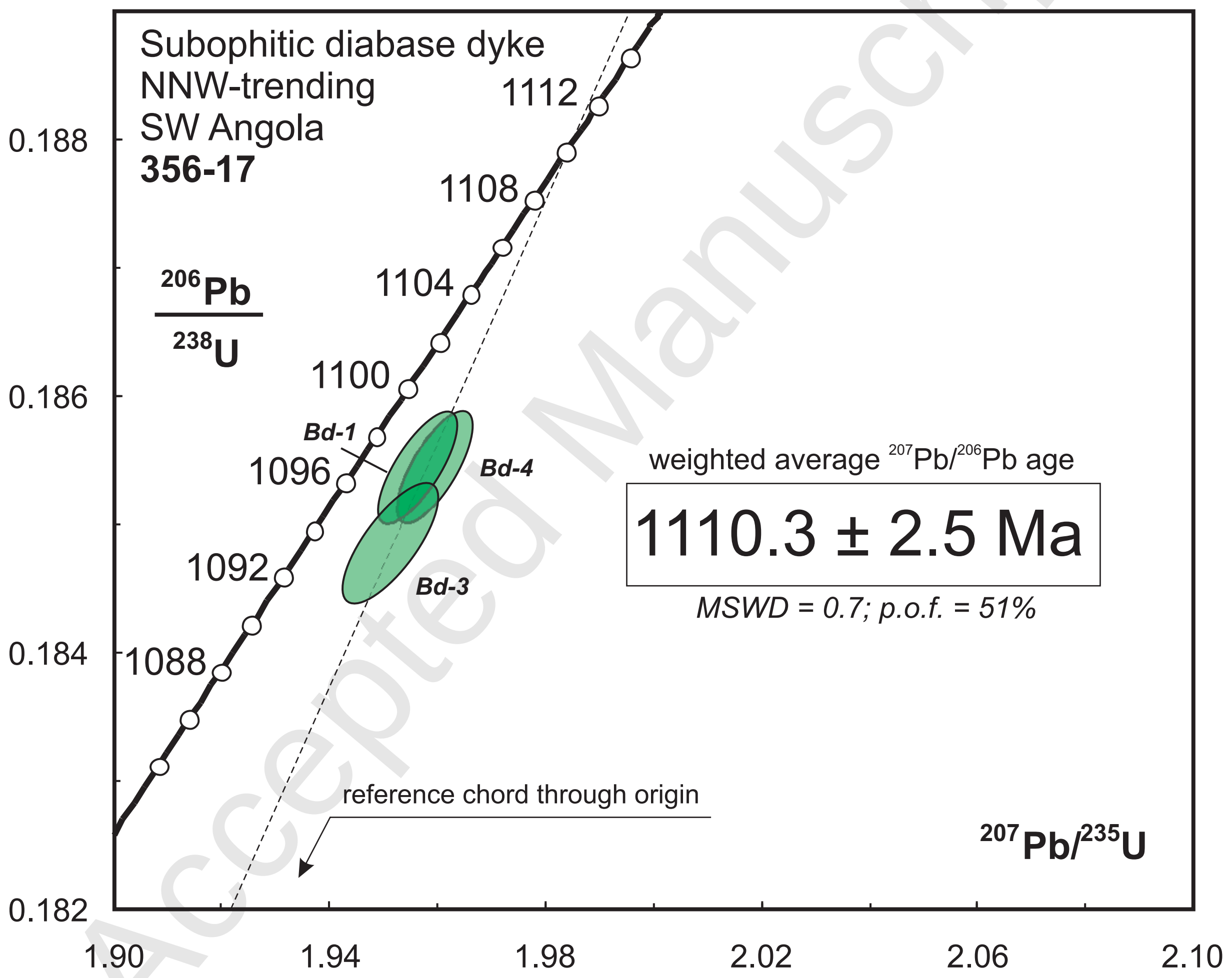
Subophitic diabase dyke
NNW-trending
SW Angola
356-17
206Pb/238U
207Pb/235U
1088
1092
1096
1100
1104
1108
1112
Bd-1
Bd-3
Bd-4
weighted average 207Pb/206Pb age
1110.3 ± 2.5 Ma
MSWD = 0.7; p.o.f. = 51%
reference chord through origin
0.182
0.184
0.186
0.188
1.90
1.94
1.98
2.02
2.06
2.10

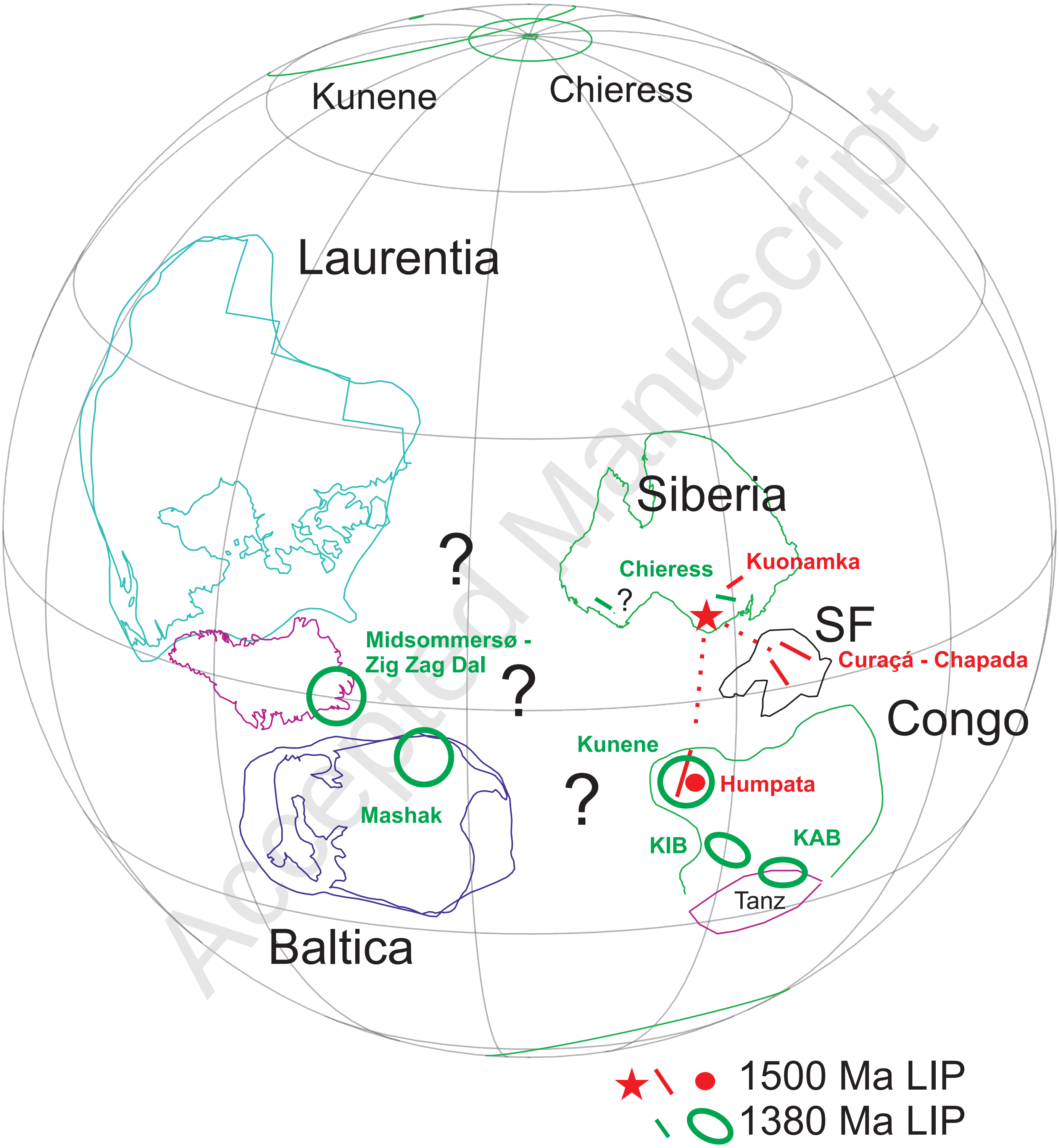
Kunene
Chieress
Laurentia
Siberia
Chieress
?
Kuonamka
SF
Curaçá - Chapada
Congo
Midsommersø -
Zig Zag Dal
?
?
Kunene
Humpata
?
Mashak
KIB
KAB
Tanz
Baltica
Accepted Manuscript
1500 Ma LIP
1380 Ma LIP

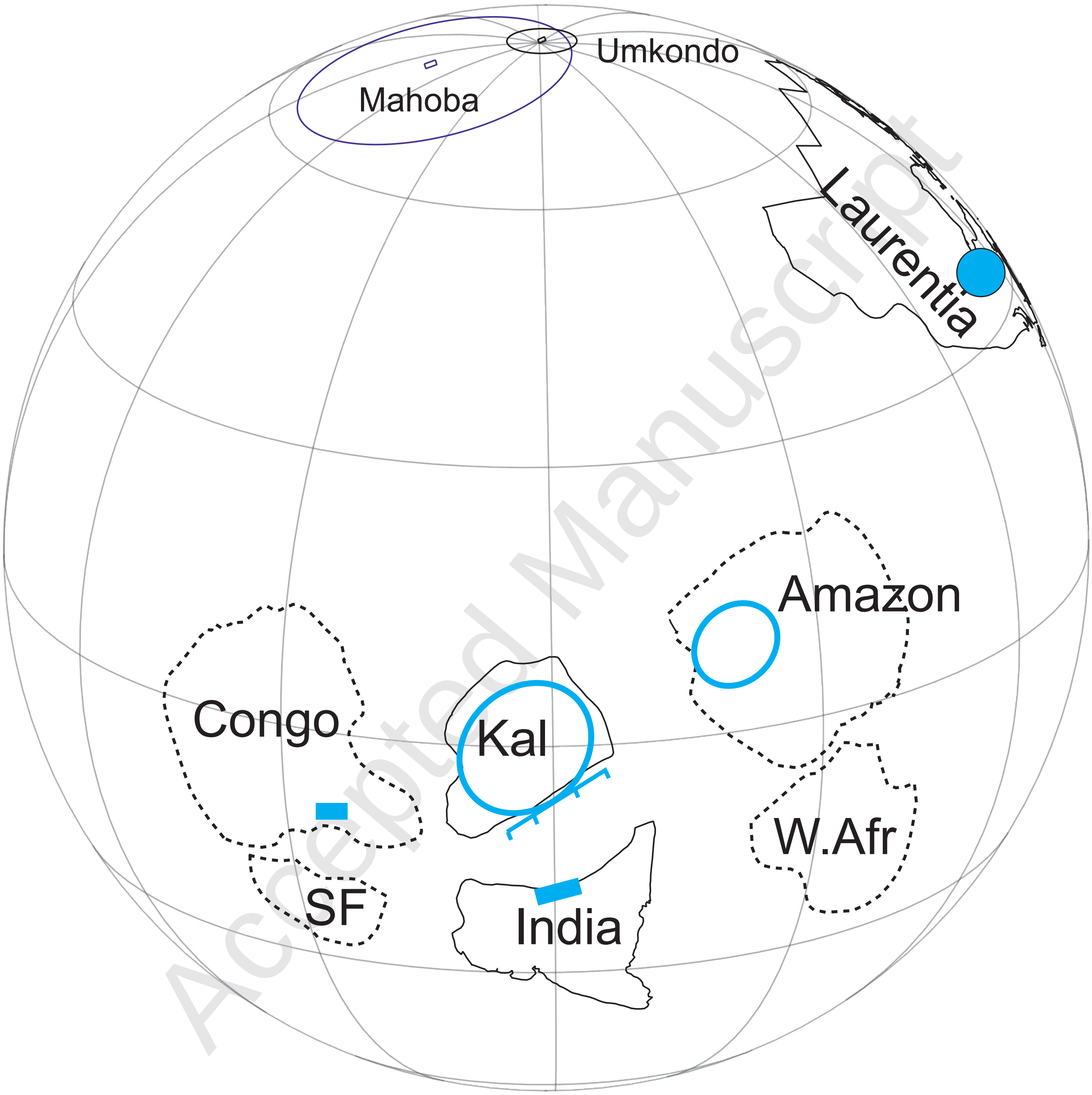

Umkondo
Mahoba
Laurentia
Amazon
Congo
Kal
W.Afr
SF
India